Descriptive Project Report

NOAA Seamless Topobathy Digital Elevation Model Pilot Incorporating Satellite-Derived Bathymetry | Kachemak, Teller, & Point Hope, Alaska

1305M223FNCNP0283 – DPR | 26 March 2024
Final Report

NOAA

Document Control

Document Information

Document Title	Descriptive Project Report
Project Title	The Generation of a Seamless Topo-Bathy DEM
TCarta Project No.	PN23014
TCarta Document No.	PN23014-DPR
External Project Number (From AXIM)	1305M223FNCNP0283
Issue Number	[05]
Issue Status	Final Report Revision 03

Client Information

Client	NOAA's Office for Coastal Management
Client Address	263 13th Ave S., St. Petersburg, FL-33701
Client Contact	Dave Stein

Revision History

Issue	Date	Status	Comments on Content	Prepared By	Checked By	Approved By
00	27 November 2023	Draft	Internal Review	TWM	CG	TWM
01	29 November 2023	Draft	First Release	TWM	CG	TWM
02	20 December 2023	Final	Second Release	TWM	CG	TWM
03	08 January 2024	Revision 01	Third Release	TWM	RS	TWM
04	24 January 2024	Revision 02	Fourth Release	TWM		TWM
05	26 March	Revision 03	Fifth Release	TWM		TWM

Project Team

Initials	Name	Role
AB	Alec Biles	Satellite Derived Bathymetrist
RS	Ross Smith	Senior Geospatial Scientist
NT	Natalie Treadwell	Satellite Derived Bathymetrist
CI	Chris Ilori	Senior Remote Sensing Scientist
TM	Tiziana Munene	Project Manager

Table of Contents

Figures in the Main Text

Tables in the Main Text

Abbreviations

AMEC	Alaska Mapping Executive Committee
AOI	Area of Interest
CHS	Canadian Hydrographic Service
CUDEM	Continuously Updated Digital Elevation Model
DEM	Digital Elevation Model
DSF	Dark Spectrum Fitting
EEZ	Exclusive Economic Zone
ERTDM	Ellipsoidally Referenced Tide Datum Model
ERZT	Ellipsoid Referenced Zoned Tides
GMT	Generic Mapping Tools
ICESat-2	Ice, Cloud and land Elevation Satellite
iFSAR	Interferometric Synthetic Aperture Radar
OIP	Inherent Optical Properties
LiDAR	Light Detection and Ranging
MAE	Mean Absolute Error
ME	Mean Error
MLLW	Mean Lower Low Water
MSE	Mean Square Error
NAD 83	North American Datum of 1983
NAVD 88	North American Vertical Datum of 1988
NIR	Near InfraRed
NGDC	National Geophysical Data Center

NOAA	National Oceanic and Atmospheric Administration
NWLON	National Water Level Observation Network
OCM	Office for Coastal Management
PFM	Pure File Magic
PMVD	Poor Man's Vertical Datum
RF	Random Forest
RMSE	Root Mean Square Error
Rrs	Remote Sensing Reflectance
RTM	Radiative Transfer Method
SDB	Satellite Derived Bathymetry
SOW	Statement of Work
SWIR	ShortWave InfraRed
TCARI	Tidal Constituent and Residual Interpolation
TOA	Top of Atmosphere
TSS	Topography of the Sea Surface
USGS	United States Geological Survey
UTM	Universal Transverse Mercator
V-Datum	Vertical Datum

1.0 Area Surveyed

The survey is in Alaska and covers three areas: Kachemak, Teller, and Point Hope.

Kachemak lies in the southwestern part of the Kenai Peninsula. It is characterized by extensive tidal flats, braided drainage, and marshlands. The seafloor in the South side of Kachemak Bay is composed of sand, gravel, rocky shores and submerged forests of kelp. The North side, including the Homer Spit, is composed primarily of gravel and sand.

Teller lies northwest of Nome on the Seward Peninsula, along the Bering Sea. The seafloor is characterized by a mix of relatively shallow areas, sedimentary deposits, and rugged, uneven terrain due to geological shifts and formations.

Point Hope lies in the northwestern end of the Lisburne Peninsula, on the Chukchi Sea. The seafloor is characterized by a sandy bottom. The area experiences strong currents that result in large shifts in its coastal bathymetry, due to erosion in an already shallow area. The shallow shelf gradually deepens into the Arctic Ocean basin.

1.1 Survey Limits

The survey limits were acquired in accordance with the requirements in the project's statement of work (SOW).

1.1.1 Kachemak

Data were to be acquired and gridded within the following survey limits, to cover a total of 971 square kilometers:

Northeast Limit	Southwest Limit
150° 53' 4.77"W 59° 46' 39.45"N	151° 48' 15.95"W 59° 27' 35.55"N

Table 1: *Kachemak survey limits*
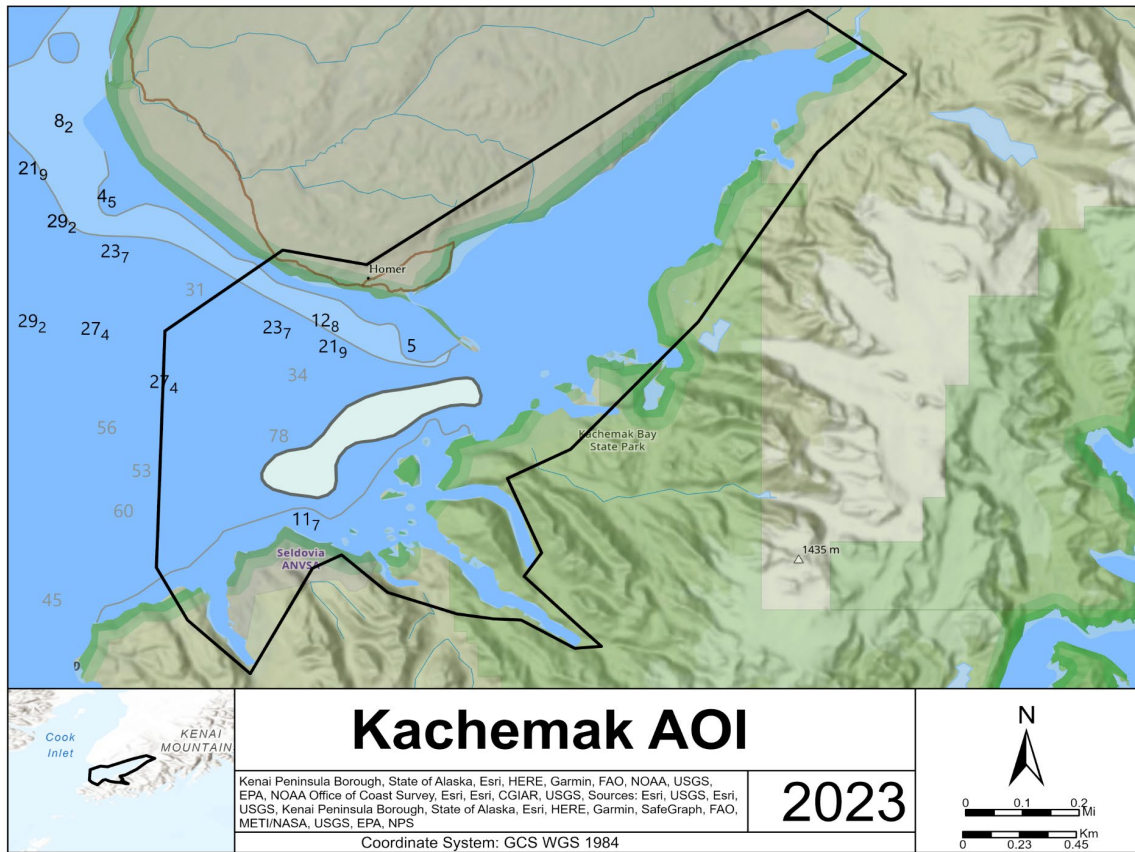
Figure 1: *Kachemak AOI*

1.1.2 Teller

Data were to be acquired and gridded within the following survey limits, to cover a total of 1,165 square kilometers:

Eastern Limit	Western Limit
166° 00' 47.71"W 65° 13' 54.65"N	167° 07' 57.22"W 65° 07' 28.05"N

Table 2: *Teller survey limits*
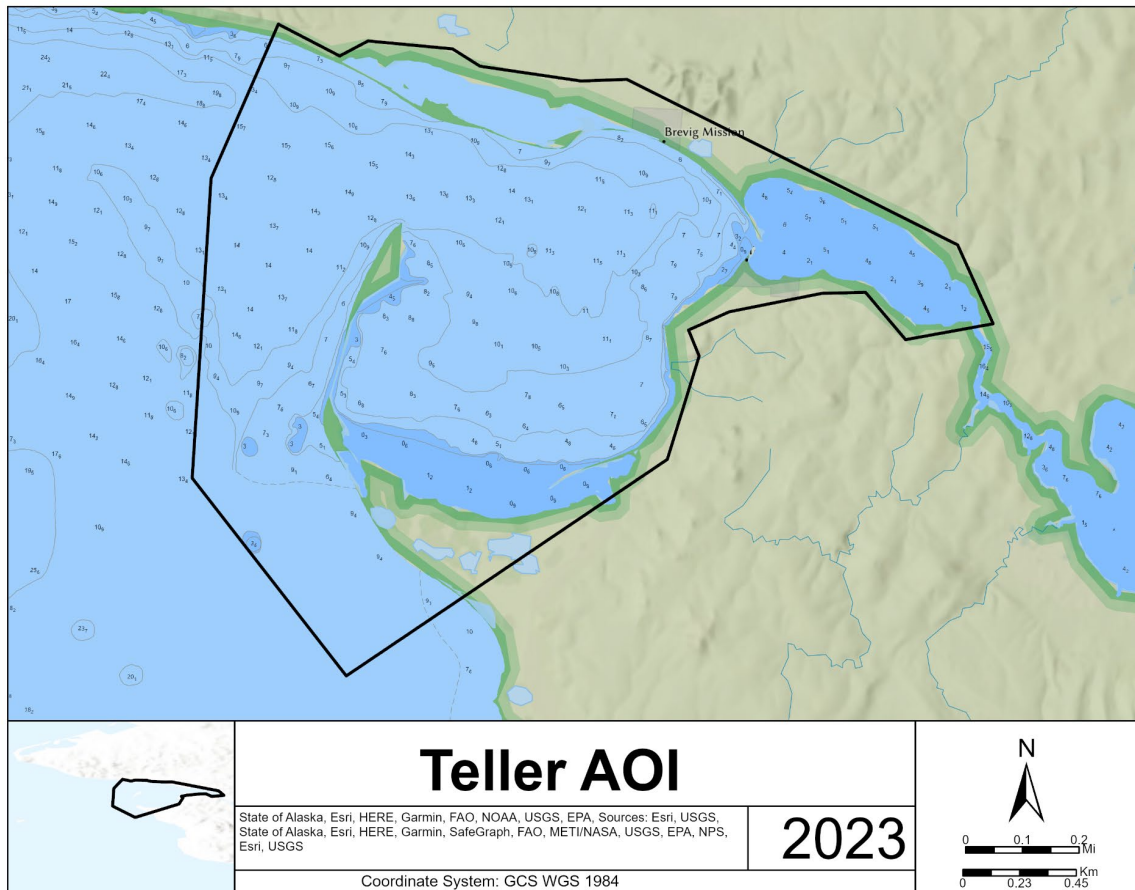
Figure 2: *Teller AOI*

1.1.3 Point Hope

Data were to be acquired and gridded within the following survey limits, to cover a total of 2,329 square kilometers:

Northwest Limit	Southeast Limit
167° 09' 7.89"W 68° 30' 18.77"N	165° 55' 47.53"W 68° 09' 24.87"N

Table 3: *Point Hope survey limits*
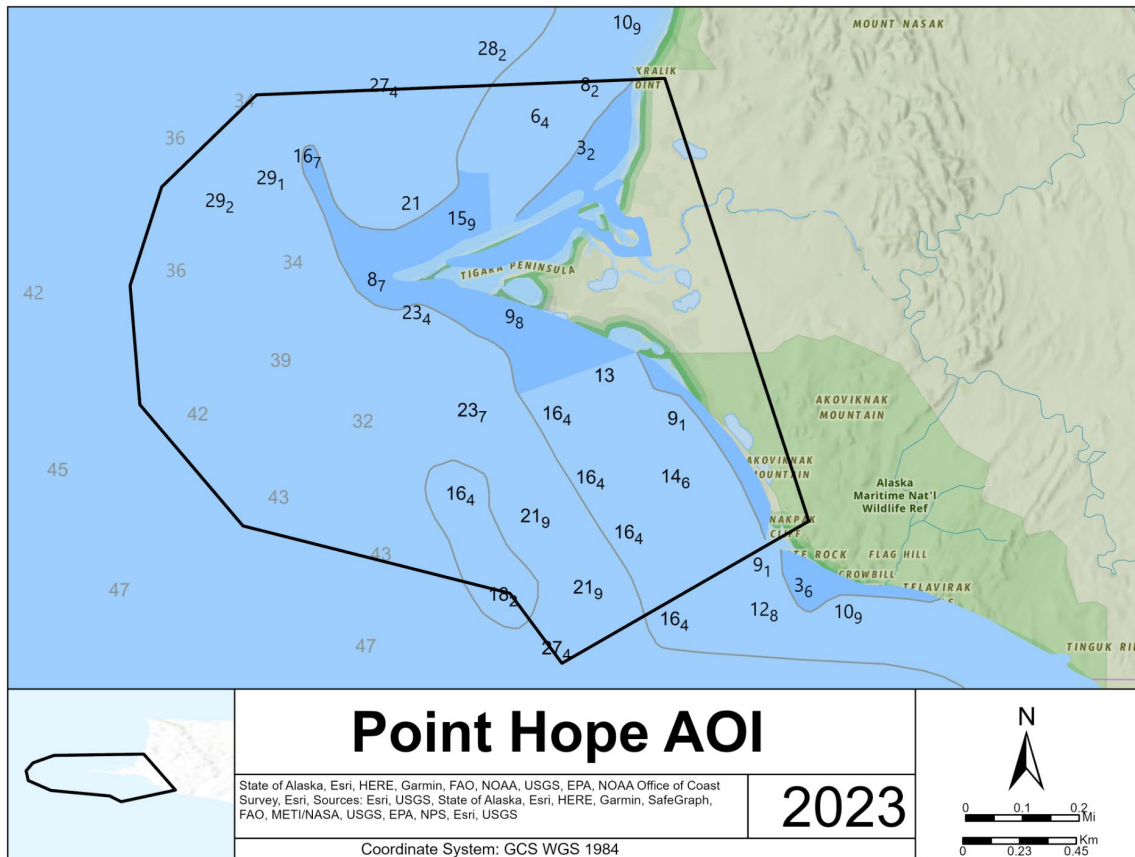
Figure 3: *Point Hope AOI*

1.2 Survey Purpose

The primary objective of this project was to fill bathymetric data gaps according to the Alaska Mapping Executive Committee (AMEC). This objective was to be achieved through:

1. Acquiring new Satellite Derived Bathymetric (SDB) data in the assigned area of interest (AOI), with the goal of expanding bathymetric data coverage beyond the current coverage from sonar and LiDAR datasets.
2. Creating a seamless topobathymetric digital elevation model (DEM) using existing topobathymetric LiDAR, sonar bathymetry, terrestrial LiDAR, Interferometric Synthetic Aperture Radar (iFSAR), and TCarta's SDB data. Minimal interpolation was to be utilized during the DEM production.

This was a pilot project to demonstrate how SDB can be used to fill in data gaps in hard to map areas due to accessibility, prohibitive cost associated with ship-based and LiDAR surveys, narrow windows of opportunities to perform survey work due to environmental and harsh weather conditions, and potential risks to operators surveying in these remote and unsurveyed

areas. Ship-based surveys are also limited in access as surveys are completed to a ~3m demarcation line, with high versus low tide data acquisition opportunities coming into play when collecting data in the shoals. On the other hand, the quality of topobathymetric LiDAR surveys is subject to suspended sediment in the water column. Due to their prohibitive cost and dependency on near perfect weather conditions, topobathymetric LiDAR surveys are not collected frequently, thus it is hard to reacquire data in areas that present as having high sediment suspension at the time of data analysis.

Given these constraints associated with ship-based and LiDAR surveys, SDB can be viewed as the 'glue' between hydrographic and terrestrial survey datasets as satellite remote sensing offers the potential for regular and wide scale imagery collection of any location at a reasonable cost. SDB also proved to be crucial in providing current bathymetry data for areas that had outdated data, as current ICESat-2 bathymetry data (collected in 2022) were also used to calibrate the SDBs.

Data from this project will be crucial to the local communities when it comes to maritime navigation, emergency response, and land management.

1.3 Survey Quality

The SDB data is adequate to fill the existing data gaps. ICESat-2 and existing in-situ bathymetry data were used to calibrate TCarta's physics-based algorithms to produce the SDB, as described in section 3.5.

1.4 Survey Coverage

The resulting DEMs from each AOI meet the coverage requirements as assigned in the SOW (Table 1-3 and Figure 1-3). Section 7.1 discussed the resulting coverage from this survey.

1.5 Survey Statistics

The following table represents the square kilometers uniquely covered by each data type contributing to each AOI's DEM.

Data Type	Unique Areal Contribution (km²)			Total (km²)
	Kachemak	Teller	Point Hope	
SDB	9.68	131.55	1.51	142.74
Sonar (Single- & Multibeam)	0.91	60.21	73.18	134.3
Topobathymetric LiDAR	42.11	36.63	1.94	80.68
Terrestrial LiDAR	93.15	N/A	66.13	159.28
iFSAR	41.47	39.05	56.36	136.88
Interpolation	825.42	893.25	2093.16	3811.83
Total Coverage	1012.74	1160.69	2292.28	4465.71

Table 4: *Survey statistics showing coverage attributed to each bathymetry source*

2.0 Source of Imagery

Imagery was selected from the Maxar WorldView and GeoEye, and Planet imagery archives, with the best and most recently available imagery being given priority.

2.1 Selection Process

Candidate images were manually reviewed and interpreted for suitability for SDB processing based on visual inspection of environmental conditions. These conditions primarily included cloud cover and cloud shadows, glint/solar glare, and water turbidity.

	Kachemak Bay	Teller	Point Hope
Maxar WorldView/GeoEye Imagery	9	8	5
Planet Imagery	9	2	2

Table 5: *Summary of images downloaded for SDB Production*

2.1.1 Kachemak

There were nine Maxar and nine Planet images that were ordered for initial reviewing and processing. Upon receipt of the full resolution imagery, the images were further ranked for image quality and production prioritization. A total of 10 images were processed through the

random forest SDB algorithm (refer to section 3.5) stage, with seven images being selected for final processing and completion. There are images that went through the SDB algorithm that were rejected from final delivery due to overlap or data quality issues like turbidity and glint.

Image ID	Sensor Platform	Acquisition Date	Acquisition Time (UTC)	Cloud Cover	Off Nadir View Angle (°)	Sensor Azimuth Angle (°)	Sun Azimuth Angle (°)	Sun Elevation Angle (°)
KB006_19MAY24 213103_0159644 90020	WorldView-2	2019-05-24	21:31:03	0.1	21.9	171.3	167.7	51.1
KB007_18SEP202 20652_01596451 8020	WorldView-3	2018-09-20	22:06:52	23.3	21.7	315.7	182.1	31.8
KB010_20220528 _205535_39_248 e	PlanetScope 248e	2022-05-28	20:55:35	0.0	1.0	111.9	155.6	50.1
KB011_20220528 _205537_71_248 e	PlanetScope 248e	2022-05-28	20:55:38	0.0	1.0	111.8	155.4	50.2
KB014_20210725 _212631_67_241 3	PlanetScope 2413	2021-07-25	21:26:32	54.0	5.0	283.4	161.8	48.7
KB016_20190415 _210434_66_105 e	PlanetScope 105e	2019-04-15	21:04:35	2.0	2.0	108.7	160.9	39.2
KB017_20190415 _210436_69_105 e	PlanetScope 105e	2019-04-15	21:04:37	0.0	2.0	108.4	160.8	39.3

Table 6: *Summary of source images that contributed to the SDB produced in the Kachemak AOI*

2.1.2 Teller

There were eight Maxar and two Planet images that were ordered for initial reviewing and processing. Upon receipt of the full resolution imagery, the images were further ranked for image quality and production prioritization. A total of eight images were processed through the SDB algorithm stage, with six images being selected for final processing and completion. There were images that went through the SDB algorithm that were rejected from final delivery due to overlap or data quality issues like turbidity and glint.

1305M223FNCNP0283 – The Generation of a Seamless Topo-Bathy DEM   NOAA

Image ID	Sensor Platform	Acquisition Date	Acquisition Time (UTC)	Cloud Cover	Off Nadir View Angle (°)	Sensor Azimuth Angle (°)	Sun Azimuth Angle (°)	Sun Elevation Angle (°)	Spatial Resolution (m)
CT002_17AUG10224336_ 015964490060	WorldView-2	2017-08-10	22:43:36	17.4	13.7	92.5	170.7	39.7	2
CT004_15JUN18230235_ 015964490010	WorldView-2	2015-06-18	23:02:35	0.0	9.0	334.2	178.3	48.1	2
CT005_22JUL13225152_0 15964490040	WorldView-2	2022-07-13	22:51:52	0.3	1.7	131.2	173.3	46.3	2
CT008_20220802_214139 _14_2465	PlanetScope 2465	2022-08-02	21:41:39	0.0	5.0	288.3	150.7	39.8	3
CT009_20220802_222058 _91_241c	PlanetScope 241c	2022-08-02	22:20:59	0.0	3.0	108.9	164.1	41.8	3
CT010_20JUN16223135_ 015964489010	GeoEye-1	2020-06-16	22:31:35	17.4	18.4	81	167.7	47.6	2

Table 7: *Summary of source images that contributed to the SDB produced in the Teller AOI*

2.1.3 Point Hope

There were five Maxar and two Planet images that were ordered for initial reviewing and processing. Upon receipt of the full resolution imagery, the images were further ranked for image quality and production prioritization. A total of five images were processed through the SDB algorithm stage, with four images being selected for final processing and completion. There were images that went through the SDB algorithm that were rejected from final delivery due to overlap or data quality issues like turbidity and glint.

Image ID	Sensor Platform	Acquisition Date	Acquisition Time (UTC)	Cloud Cover	Off Nadir View Angle (°)	Sensor Azimuth Angle (°)	Sun Azimuth Angle (°)	Sun Elevation Angle (°)	Spatial Resolution (m)
PH002_15JUN22224053_015964518010	WorldView-3	2015-06-22	22:40:53	0.0	20.9	66.1	171.6	45.2	2
PH004_19JUN12230727_016009834020	WorldView-2	2019-06-12	23:07:27	0.0	24.0	25.4	180.2	45	2
PH006_20230828_215552_89_24af	PlanetScope 24af	2023-08-28	21:55:53	0.0	1.6	115.2	159.5	30.1	3
PH007_20230923_215802_19_24c7	PlanetScope 24c7	2023-09-23	21:58:02	0.0	2.8	288.2	163.4	20.6	3

Table 8: *Summary of source images that contributed to the SDB produced in the Point Hope AOI*

3.0 SDB Processes

3.1 Imagery Preparation

The selected images were made ready for atmospheric correction prior to SDB retrieval. Each image was subsequently loaded automatically into an in-house wrapper code where atmospheric correction was implemented.

3.2 Atmospheric Correction

Atmospheric correction was performed using ACOLITE. This is the removal of the signal at the sensor (i.e. top of atmosphere, TOA), the radiance contributions from the atmosphere and the water surface to derive the remote sensing reflectance (Rrs) - the primary input into the SDB model. The dark spectrum fitting (DSF) method, which uses the band with the lowest atmospheric path over multiple targets in the scene, was used in ACOLITE to remove unwanted signals from the TOA. To derive Rrs, ACOLITE was parameterized using its default processing options. To check for negative reflectance, the 400 - 600 nm waveband was used instead of the default 400 – 900 nm. This is to limit the loss of viable data in shallow water areas in the near infrared (NIR) band.

3.3 Glint Removal

To remove specular reflection off the sea surface (if any) in the selected images, glint correction was performed by default in ACOLITE. The glint algorithm uses the shortwave infrared (SWIR) bands to estimate residual signal from the Rrs images and then remove this from the satellite bands used for SDB modeling. Where ACOLITE glint correction failed, the Hedley method [*Hedley et al.,* 2005] was used for glint correction instead.

3.4 Tidal Correction

The in-situ and ICESat-2 data that was used to calibrate the extracted SDBs had already been corrected to the project's vertical datum [NAVD88; refer to section 4.3.1], thus no further tide corrections were applied to the final SDB surfaces.

3.5 SDB Production Methods

A 2018 study done by the Canadian Hydrographic Surveys (CHS) [*Aloha et al.,* 2018] to assess the accuracy of SDB techniques in mapping Canadian Arctic waters concluded that the depths obtained through satellite remote sensing techniques are feasible to be included in charts, especially for hard to map areas that have either very old or no data. The Canadian Arctic's seafloor, remoteness, and weather conditions are comparable to those of our AOIs in Alaska, thus making SDB data acquisition the more feasible option in mapping these areas. These are the three algorithms that TCarta to produce SDBs:

3.5.1 Radiative Transfer Method (RTM)

One of the methods that TCarta uses to produce SDB is by using a radiative transfer model. This model relates the Rrs to the inherent optical properties (IOP) of water, that is, absorption and backscatter properties of the water column, the bottom reflectance, and water depth. As such, this method does not rely on ground truth or other calibration data to produce SDB results. For each pixel in the satellite image, the algorithm finds the environmental characteristics, that is, the water IOPs, that produce the simulated color that most closely matches the one observed in the pixel. The algorithm then assigns the water depth value that is part of those environmental characteristics to that pixel. Apart from IOPs, this model also considers the solar zenith and azimuth angles, and the sensor zenith and azimuth angles, which are all available in the satellite image metadata.

3.5.2 Random Forest (RF)

For this supervised machine learning method, the calibration depth dataset acts as the dependent variable and each spectral band and every band-ratio permutation that exists for that satellite sensor are used as independent variables. The random forest method is different from the traditional log-ratio method in that it incorporates information from all spectral bands, not just green and blue bands. With minimal training, the algorithm determines which spectral bands have the most statistical correlation with the trained model to produce the most accurate water depths. Bathymetry data derived from the ICESat-2 space-based sensor and other in-situ bathymetry were used to train the model. The ICESat-2 bathymetry data are produced by a completely independent satellite, sensor and derivation method for calculating water depths from space-based instruments.

3.5.3 Band Ratio (BR)

This is the most common empirically driven SDB method, which models the relationship between seafloor reflectance and depth utilizing the natural-log ratio of the blue band and green band of multispectral imagery and point calibration bathymetry data. TCarta typically will utilize a combination of ICESat-2 bathymetry and other available in-situ sources as calibration data. A regression is plotted against the depth-to-reflectance relationship, then an analyst can remove outlier points which are negatively contributing to the correlation. Once a final regression is calculated, the formula is applied to the entire band-ratio raster to derive a continuous depth surface.

For this project, the resulting SDBs were produced using the RF method, apart from PH002_15JUN22224053_015964518010, where the RTM method was utilized. None of the available bathymetry data intersected with the image in this part of Point Hope.

3.6 Data Cleaning

During post-processing, SDB surfaces were visually inspected alongside satellite imagery, nautical charts, ICESat-2 bathymetry and in-situ bathymetry to remove spurious points and errors in depths due to:

- Clouds/Shadows
- Turbidity
- Whitecaps, whitewash, excessive waves
- Boats/wakes
- Areas predicted too shallow or too deep due to turbidity or dark objects
- Depths beyond optically shallow extents / pixels on land
- Any other erroneous depths

Further interrogation in a 3D environment ensured erroneous points due to turbidity, glint and other detractors from SDB quality were removed from the data using point cloud editing software, Pure File Magic (PFM).

3.7 Validation Method

Each resulting SDB surface was evaluated individually with the ICESat-2 and other in-situ bathymetry data to assess the data accuracy of each iteration of SDB processing for each image (the ICESat-2 and other in-situ bathymetry depth values were combined to form a single set of calibration data). Draft SDB surfaces that failed the statistical comparison or could be improved upon were identified for reprocessing. Accuracy statistics were used to compare accuracy of overlapping SDB surface to select the more accurate SDB surface.

Data comparison reporting was divided into depth bins and assessed using both absolute difference and percentage of depth difference. Statistical comparison of ICESat-2 and other in-situ bathymetric depths with SDB surfaces was divided into depth bins with ranges: above 0-0m, 0-2m, 2-5m, 5-10m, 10-20m, 20-30m, and 30+m to provide more discretized comparisons. These bin spacings are ingrained in TCarta's Trident Tools algorithm. They are set up in a way that the bin sizes get wider with depth, since there are less ICESat-2 bathymetry points the deeper you go. TCarta mostly utilizes ICESat-2 data for training and validating SDB, and in cases where other bathymetry sources are available to complement ICESat-2 data, then that is utilized. Statistics were calculated for each SDB surface individually using Mean Error (ME), Mean Absolute Error (MAE), Mean Square Error (MSE) and Root Mean Square Error (RMSE). The ICESat-2 bathymetry data used in this project for SDB calibration were delivered as an ancillary dataset in the geodatabase. The SDB tabular statistics for each image are included in section 3.9.

3.8 Data Holidays

Final SDBs are subject to having data holidays in them, depending on the quality of the available imagery. Turbidity, ice cover, especially in Kachemak Bay, and clouds and cloud shadows resulted in data holidays in the SDB surfaces.

3.8.1 Imagery Gaps

Some locations with no SDB are due to of imagery unavailability. At such high latitudes, seafloor reflectance values, even when clear water conditions exist, can be <1-2%. The imagery collection window is quite short in Alaska, with only a few months of ice-free conditions in some locations. With consideration for immense volumes of sediment added to the water

column by river discharge and glacial runoff, elemental factors combined to create a higher likelihood of gaps in the image archive.

3.8.2 SDB Gaps
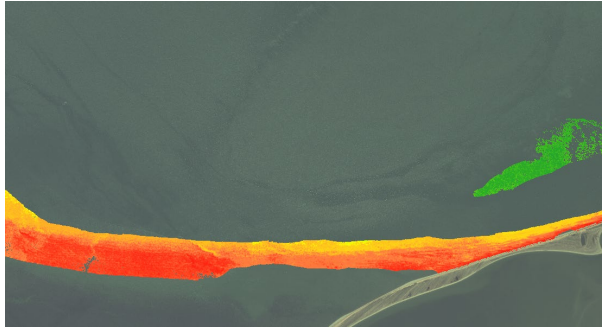
Glint	This screenshot shows an example of a location where the raw SDB surface was edited to remove inaccurate areas over glinted waters.

Figure 4: *An example of SDB gap due to glint*

Clouds and Cloud Shadows	This screenshot shows a location containing clouds and cloud shadows. The raw SDB was edited to remove inaccurate returns that occurred over the cloud shadows. These shadows present as false dark areas on the seafloor. Clouds were removed during image processing.

Figure 5: *An example of SDB gap due to clouds and cloud shadows*

Turbidity	This screenshot shows KB016 in an area where the raw SDB was edited to remove inaccurate returns due to turbidity in the water.

Figure 6: *An example of SDB gap due to turbidity*

3.9 SDB Production Summary

A total of 17 SDB surfaces were produced for the three AOIs. Below is a summary of the resulting SDB surfaces and their corresponding quality assurance and quality control statistics.

	Kachemak Bay	Teller	Point Hope
Maxar Imagery	2	4	2
Planet Imagery	5	2	2

Table 9: *Summary of images that were processed through the SDB algorithm*

KB006_19MAY24213103_015964490020

Interval	ME	MAE	MSE	RMSE	MAPE
0m - 28.89m	-0.027	2.285	5.32	2.12	19.915
0m - 1m	-2.421	2.421	10.203	3.194	72.002
1m - 5m	-0.866	1.001	2.495	1.58	18.762
5m - 10m	-1.337	1.806	6.013	2.452	18.662
10m - 15m	-0.747	2.582	10.218	3.197	20.576
15m - 20m	1.482	2.743	11.374	3.373	19.236
20m - 30m	3.878	4.046	22.415	4.734	22.718

Figure 7: *Table of statistical comparison of in-situ bathymetry and KB006 SDB surface (left); Resulting KB006 SDB surface with depths ranging from -1.29m to -7.63m (right)*

KB007_18SEP20220652_015964518020

Interval	ME	MAE	MSE	RMSE	MAPE
0m - 1.99m	-0.01	1.193	2.676	1.636	64.143

Figure 8: *Table of statistical comparison of in-situ bathymetry and KB007 SDB surface (left); Resulting KB007 SDB surface with depths ranging from 1.81m to -6.73m (right)*

KB010_20220528_205535_39_248e					
Interval	ME	MAE	MSE	RMSE	MAPE
0.7m - 2.9m	3.062	3.062	10.13	3.183	256.541
0m - 1m	0.994	0.994	1.154	1.074	540.526
1m - 5m	3.138	3.138	10.459	3.234	246.151

Figure 9: *Table of statistical comparison of in-situ bathymetry and KB010 SDB surface (left); Resulting KB010 SDB surface with depths ranging from 1.95m to -1.65m (right)*

KB011_20220528_205537_71_248e					
Interval	ME	MAE	MSE	RMSE	MAPE
0.34m - 1.63m	0.231	0.444	0.311	0.558	300.708
0m - 1m	0.242	0.471	0.341	0.584	339.318
1m - 5m	0.189	0.347	0.204	0.452	161.644

Figure 10: *Table of statistical comparison of in-situ bathymetry and KB011 SDB surface (left); Resulting KB011 SDB surface with depths ranging from 1.21m to -13.35m (right)*
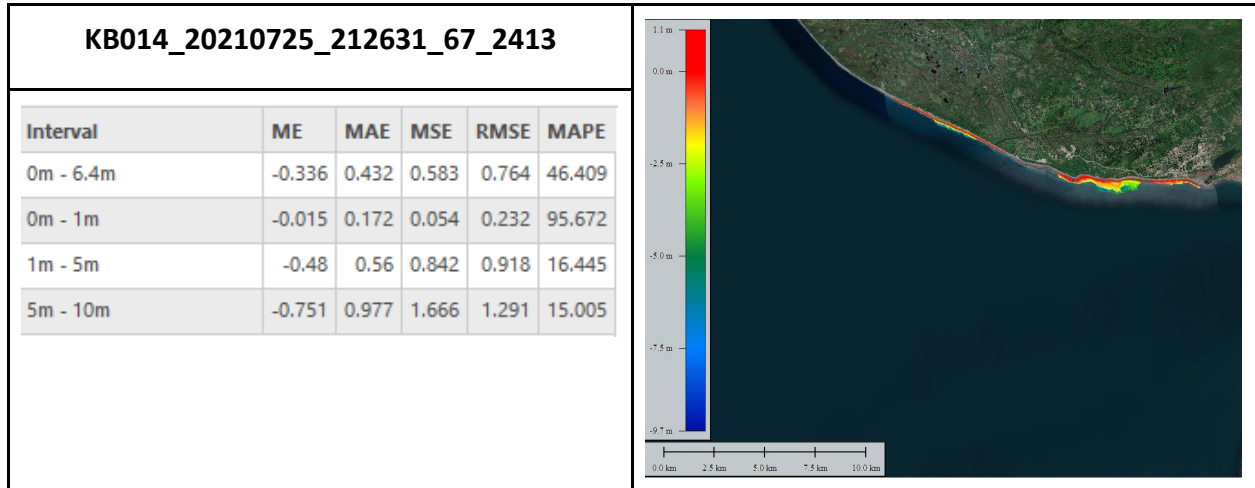
Figure 11: *Table of statistical comparison of in-situ bathymetry and KB014 SDB surface (left); Resulting KB014 SDB surface with depths ranging from 1.12m to -9.74m (right)*

KB014_20210725_212631_67_2413

Interval	ME	MAE	MSE	RMSE	MAPE
0m - 6.4m	-0.336	0.432	0.583	0.764	46.409
0m - 1m	-0.015	0.172	0.054	0.232	95.672
1m - 5m	-0.48	0.56	0.842	0.918	16.445
5m - 10m	-0.751	0.977	1.666	1.291	15.005

KB016_20190415_210434_66_105e

Interval	ME	MAE	MSE	RMSE	MAPE
0m - 12.76m	1.06	2.238	10.244	3.201	135.266
0m - 1m	-1.365	1.384	2.202	1.484	69.409
1m - 5m	0.381	0.886	1.307	1.143	88.375
5m - 10m	4.872	4.872	26.655	5.163	236.125
10m - 15m	8.606	8.606	74.353	8.623	412.493

Figure 12: *Table of statistical comparison of in-situ bathymetry and KB016 SDB surface (left); Resulting KB016 SDB surface with depths ranging from 3.42m to –3.48m (right)*

KB017_20190415_210436_69_105e

Interval	ME	MAE	MSE	RMSE	MAPE
0m - 16.88m	0.033	1.936	8.39	2.897	113.824
0m - 1m	-1.679	1.683	4.475	2.115	67.643
1m - 5m	-0.763	1.159	1.958	1.399	36.899
5m - 10m	2.581	2.581	7.974	2.824	70.928
10m - 15m	8.013	8.013	66.664	8.165	486.549

Figure 13: *Table of statistical comparison of in-situ bathymetry and KB017 SDB surface (left); Resulting KB017 SDB surface with depths ranging from 0.50m to -6.30m (right)*

3.9.2 Teller

CT002_17AUG10224336_015964490060

Interval	ME	MAE	MSE	RMSE	MAPE
0m - 6.38m	1.022	1.057	1.175	1.084	106.099
0m - 1m	-0.725	0.725	0.541	0.736	71.046
1m - 5m	1.054	1.069	1.196	1.094	107.89
5m - 10m	0.491	0.509	0.309	0.556	10.181

Figure 14: *Table of statistical comparison of in-situ bathymetry and CT002 SDB surface (left); Resulting CT002 SDB surface with depths ranging from -0.34m to -7.84m (right)*

CT004_15JUN18230235_015964490010

Interval	ME	MAE	MSE	RMSE	MAPE
0m - 6.94m	0.04	0.566	0.622	0.789	47.971
0m - 1m	-0.258	0.313	0.19	0.436	40.345
1m - 5m	0.228	0.572	0.49	0.7	37.731
5m - 10m	2.765	2.765	7.754	2.785	89.275

Figure 15: *Table of statistical comparison of in-situ bathymetry and CT004 SDB surface (left); Resulting CT004 SDB surface with depths ranging from -0.26m to -4.48m (right)*

CT005_22JUL13225152_015964490040

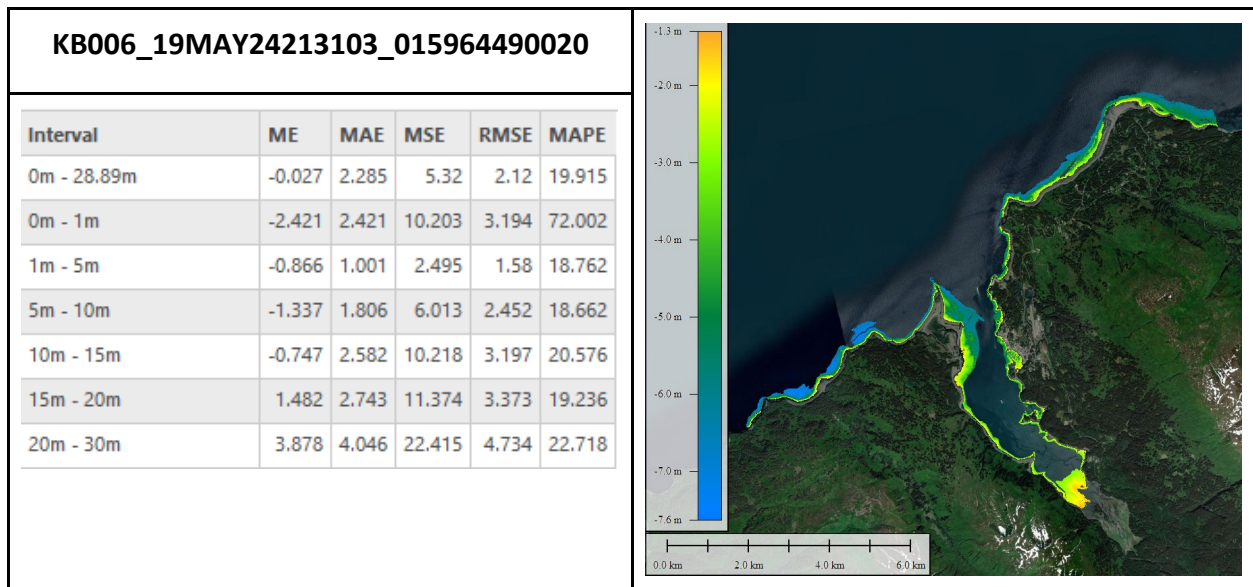| Interval	ME	MAE	MSE	RMSE	MAPE
0m - 3.84m	0.135	0.382	0.236	0.486	246.407
0m - 1m	0.158	0.265	0.113	0.336	204.834
1m - 5m	0.522	0.609	0.501	0.708	211.783

Figure 16: *Table of statistical comparison of in-situ bathymetry and CT005 SDB surface (left); Resulting CT005 SDB surface with depths ranging from 0.64m to -3.50m (right)*

1305M223FNCNP0283 – The Generation of a Seamless Topo-Bathy DEM   *NOAA*

CT008_20220802_214139_14_2465

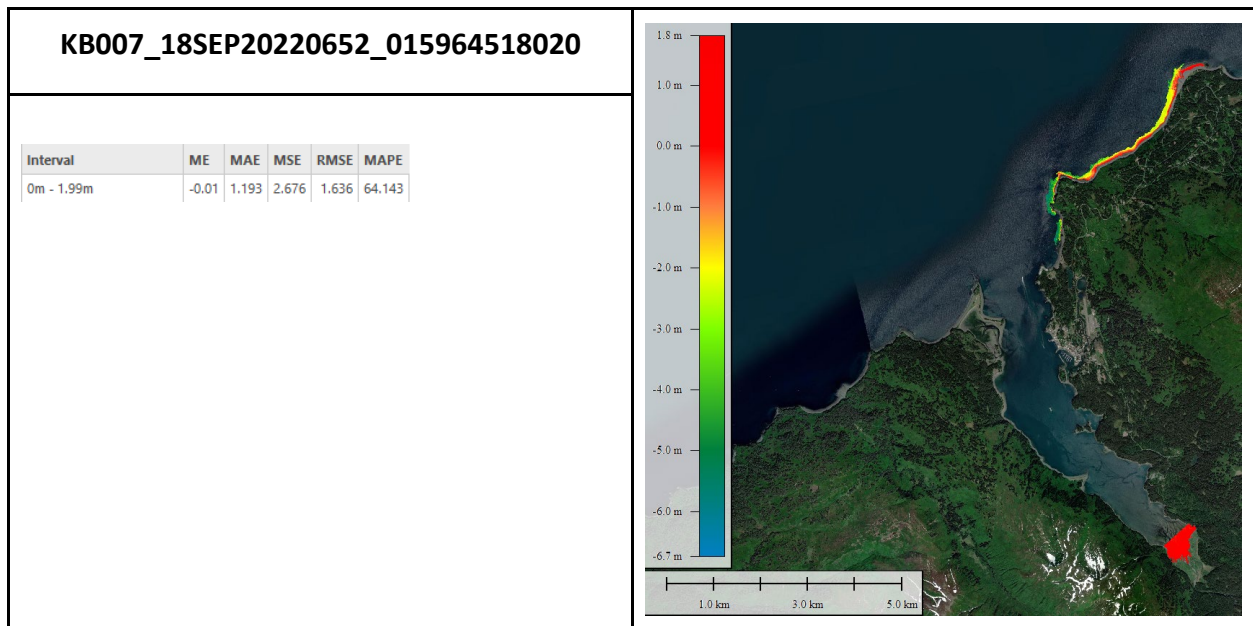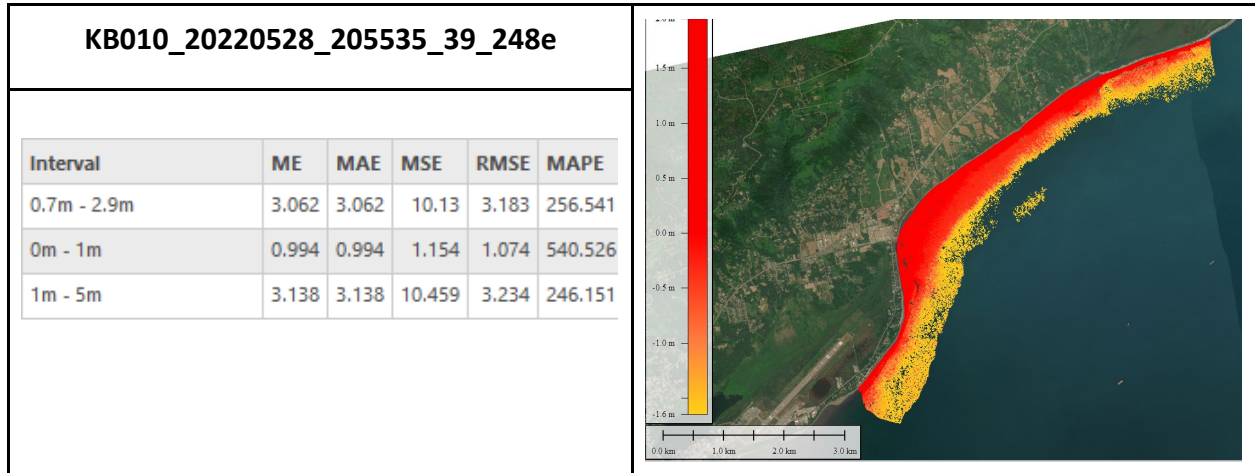| Interval	ME	MAE	MSE	RMSE	MAPE
0m - 0.54m	0.025	0.083	0.013	0.114	117.709
0m - 1m	0.094	0.172	0.042	0.205	538.832

Figure 17: *Table of statistical comparison of in-situ bathymetry and CT008 SDB surface (left); Resulting CT008 SDB surface with depths ranging from 0.91m to -1.89m (right)*

CT009_20220802_222058_91_241c

Interval	ME	MAE	MSE	RMSE	MAPE
0m - 8.91m	-0.182	0.411	0.36	0.6	194.547
0m - 1m	-0.164	0.338	0.269	0.519	170.54
1m - 5m	-0.159	0.629	0.598	0.773	59.724
5m - 10m	1.279	1.279	2.859	1.691	27.883

Figure 18: *Table of statistical comparison of in-situ bathymetry and CT009 SDB surface (left); Resulting CT009 SDB surface with depths ranging from 9.5m to -5.39m (right)*
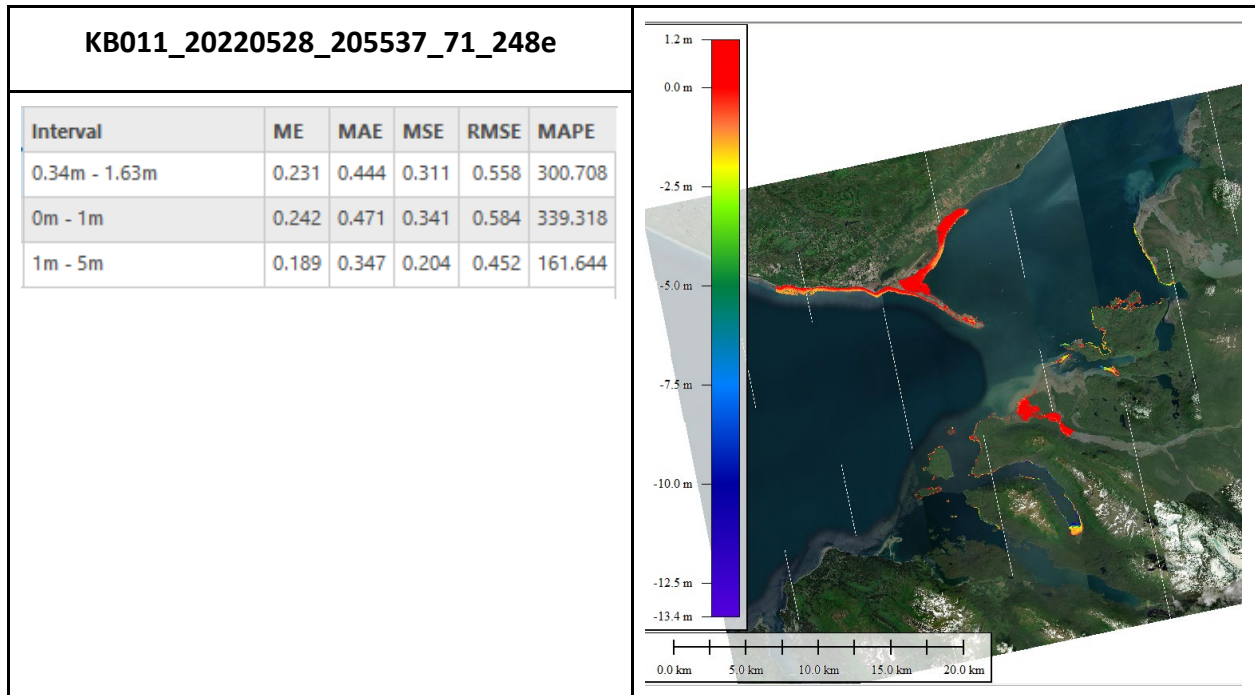
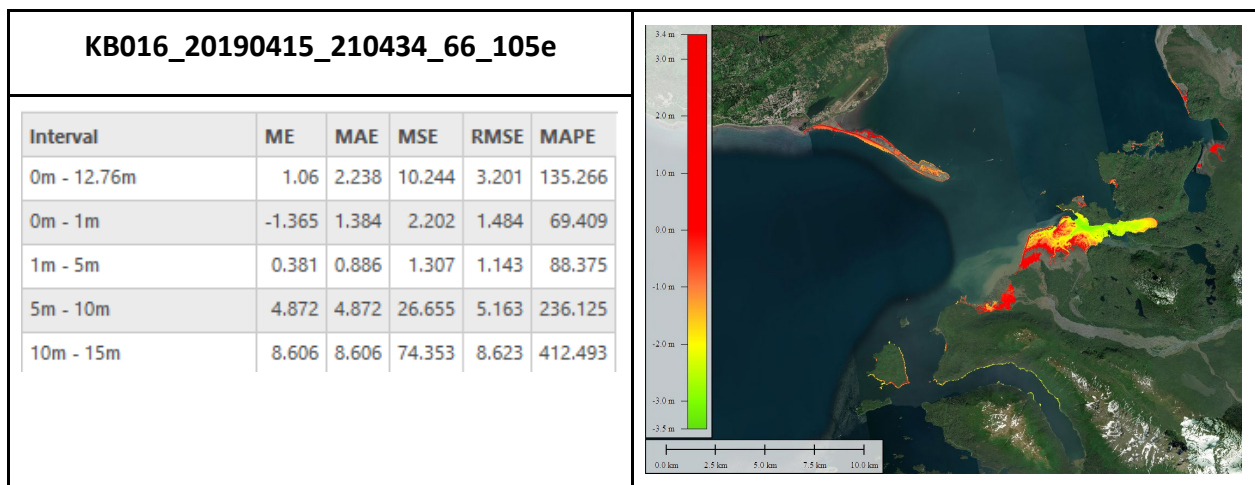| CT010_20JUN16223135_015964489010					
Interval	ME	MAE	MSE	RMSE	MAPE
0m - 27.95m	0.154	0.756	4.48	2.117	171.735
0m - 1m	-0.099	0.311	0.51	0.714	161.26
1m - 5m	-0.048	0.794	2.153	1.467	132.369
5m - 10m	-0.349	1.291	2.753	1.659	18.58
10m - 15m	2.393	2.406	8.205	2.864	24.832
15m - 20m	7.665	7.665	61.384	7.835	78.339
20m - 30m	13.774	13.774	194.547	13.948	137.913

Figure 19: *Table of statistical comparison of in-situ bathymetry and CT010 SDB surface (left); Resulting CT010 SDB surface with depths ranging from 0.99m to -11.88m (right)*

3.9.3 Point Hope

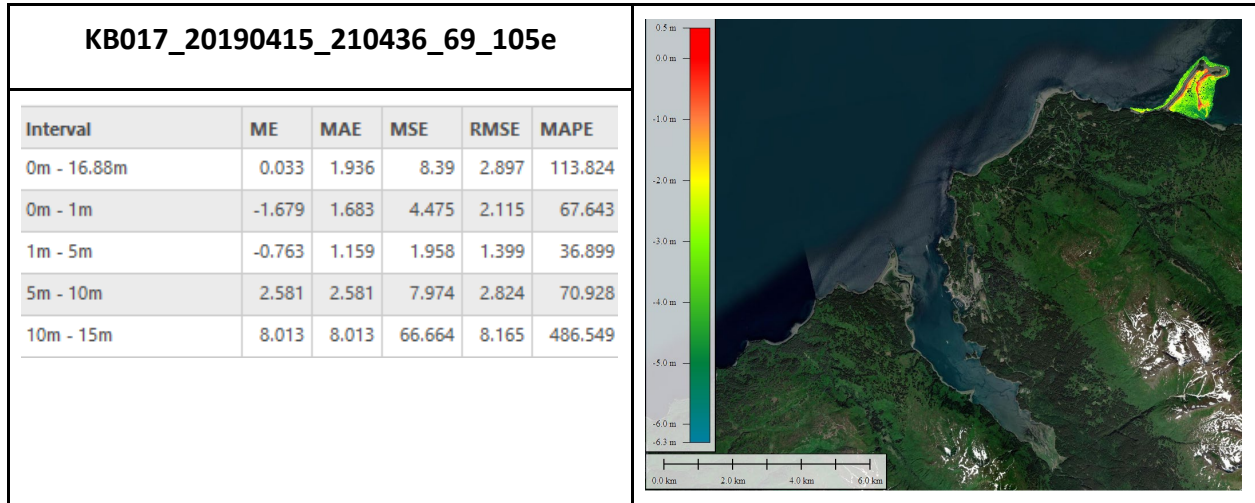| PH002_15JUN22224053_015964518010 |
|---|
| *No ICESat-2 nor any other bathymetry data intersecting the surface; this SDB was produced using the RTM method* |

Figure 20: *Table of statistical comparison of in-situ bathymetry and PH002 SDB surface (left); Resulting PH002 SDB surface with depths ranging from -1.13m to -4.49m (right)*

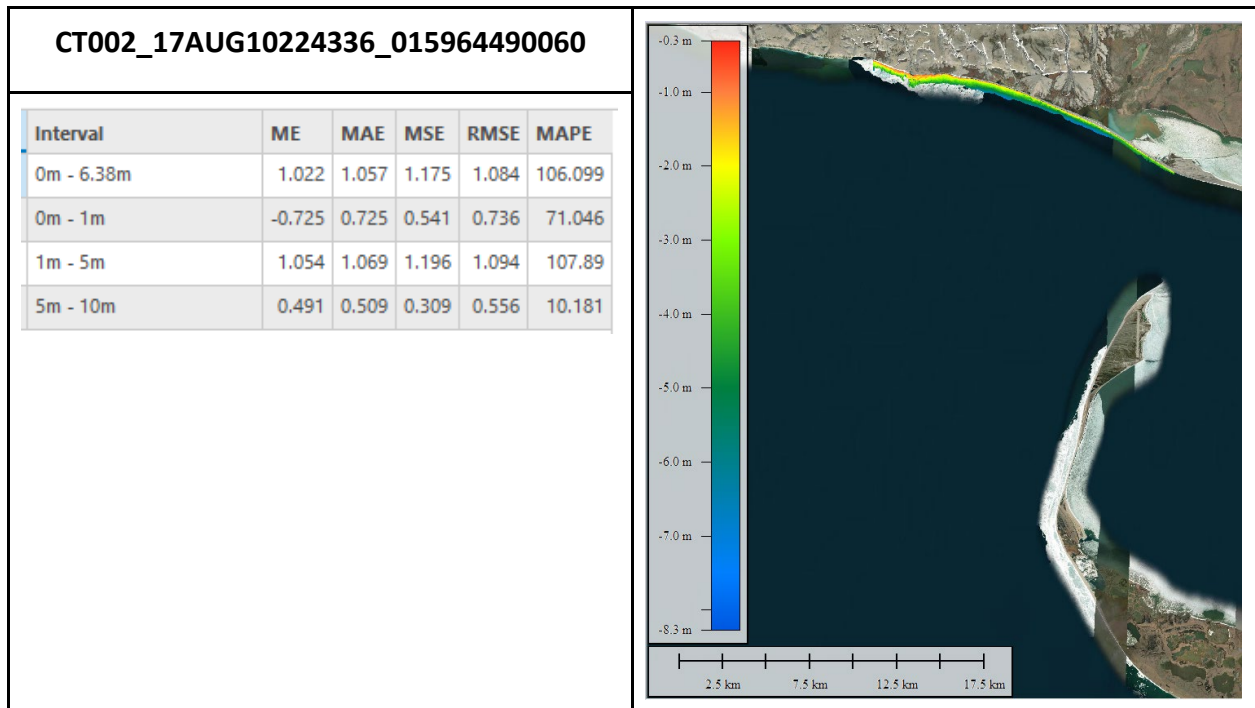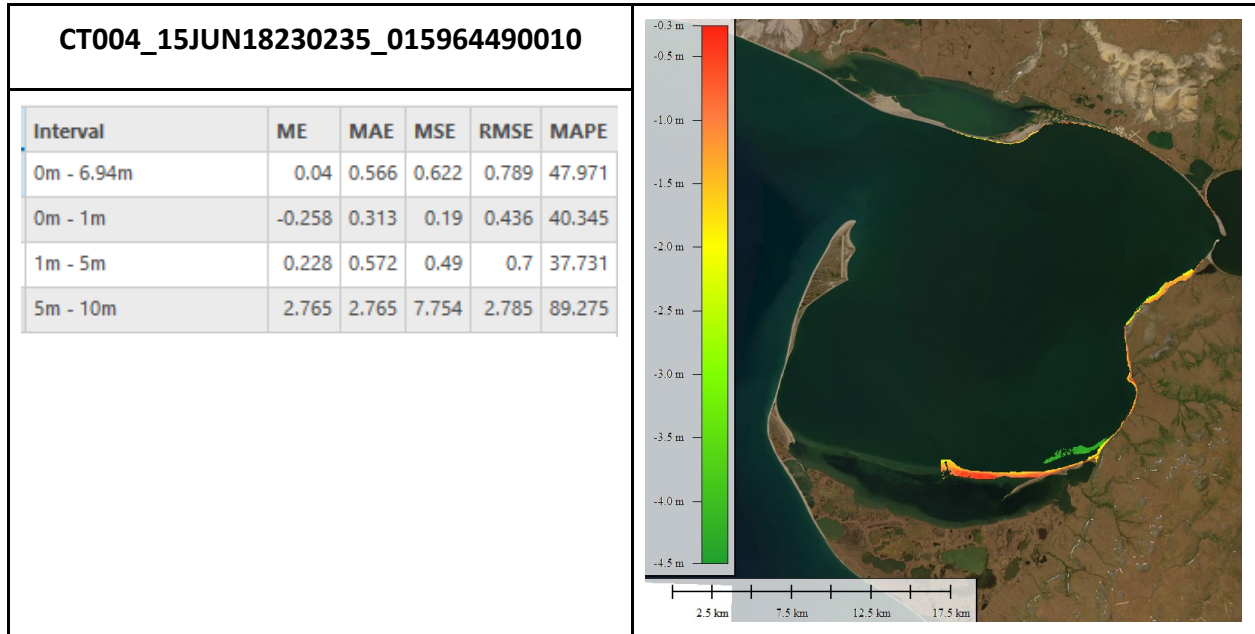| PH004_19JUN12230727_016009834020					
Interval	ME	MAE	MSE	RMSE	MAPE
0m - 0.79m	0.021	0.237	0.113	0.336	27.255
0m - 1m	0.658	0.659	0.666	0.816	478.489

Figure 21: *Table of statistical comparison of in-situ bathymetry and PH004 SDB surface (left); Resulting PH004 SDB surface with depths Ranging from 0.71m to -5.12m (right)*

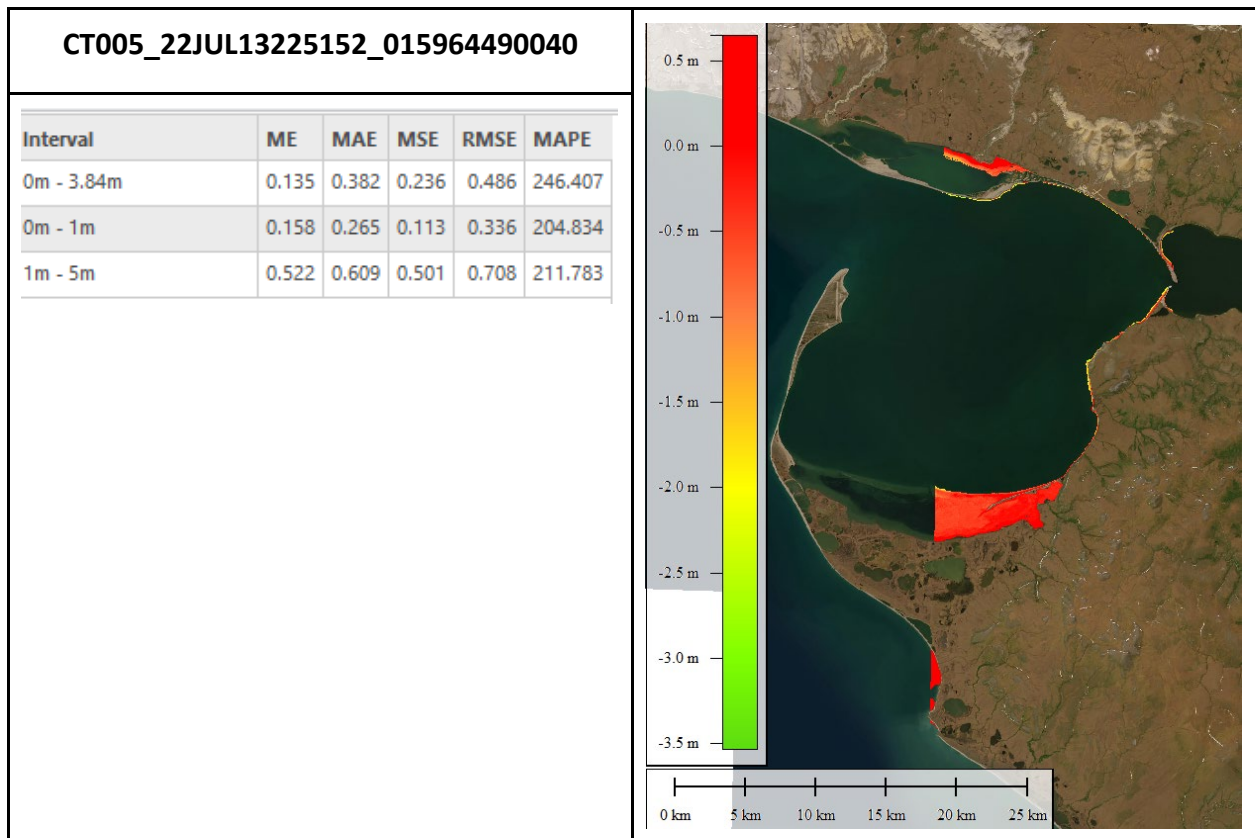| PH006_20230828_215552_89_24af							
	OID	Interval	ME	MAE	MSE	RMSE	MAPE
1	0	0m - 11.69m	-0.184	0.42	0.331	0.575	25.214
2	1	0m - 1m	-0.644	0.65	0.543	0.737	50.285
3	2	1m - 5m	-0.032	0.317	0.174	0.417	14.065
4	3	5m - 10m	2.133	2.18	5.452	2.335	70.32
5	4	10m - 15m	3.659	3.659	16.035	4.004	55.32

Figure 22: *Table of statistical comparison of in-situ bathymetry and PH006 SDB surface (left); Resulting PH006 SDB surface with depths ranging from -1.01m to -5.57m (right)*

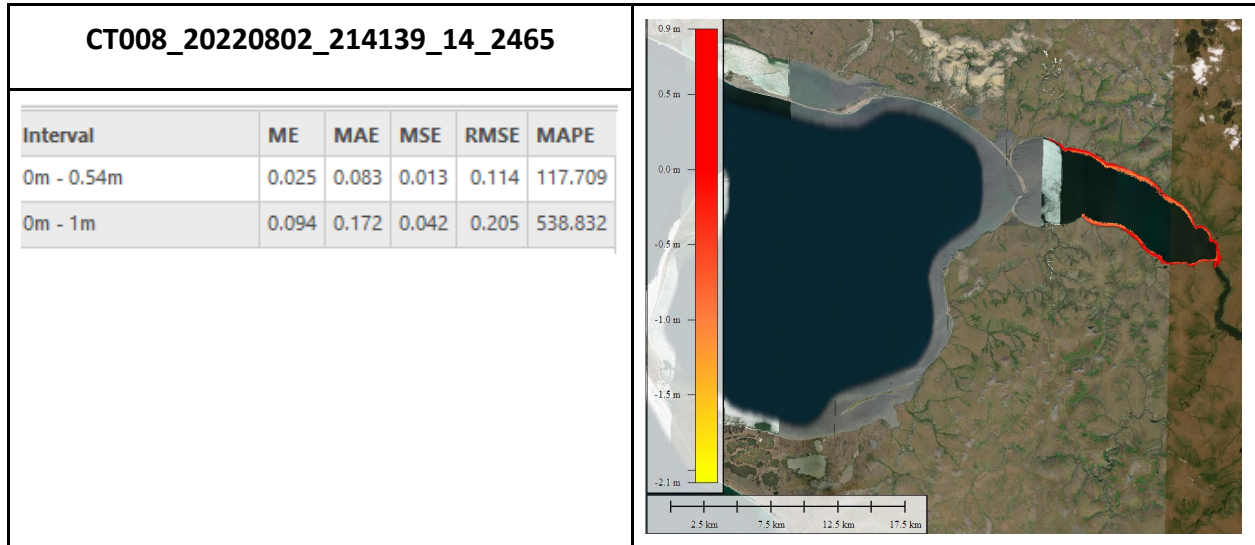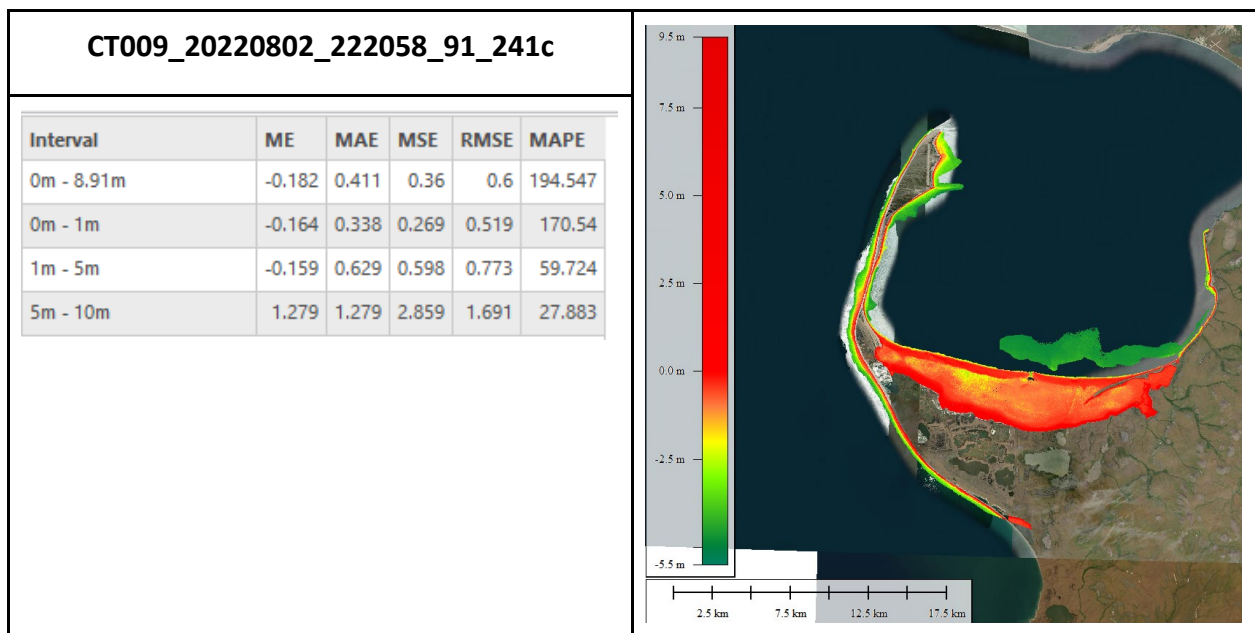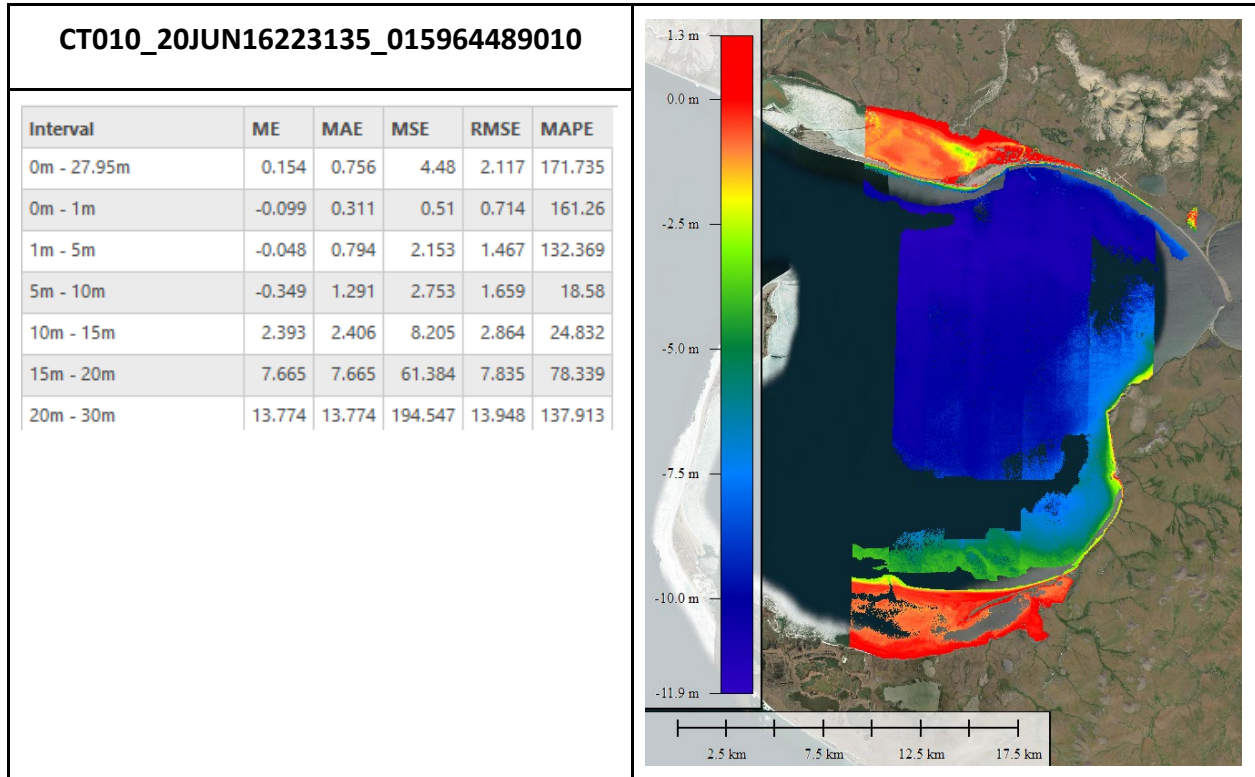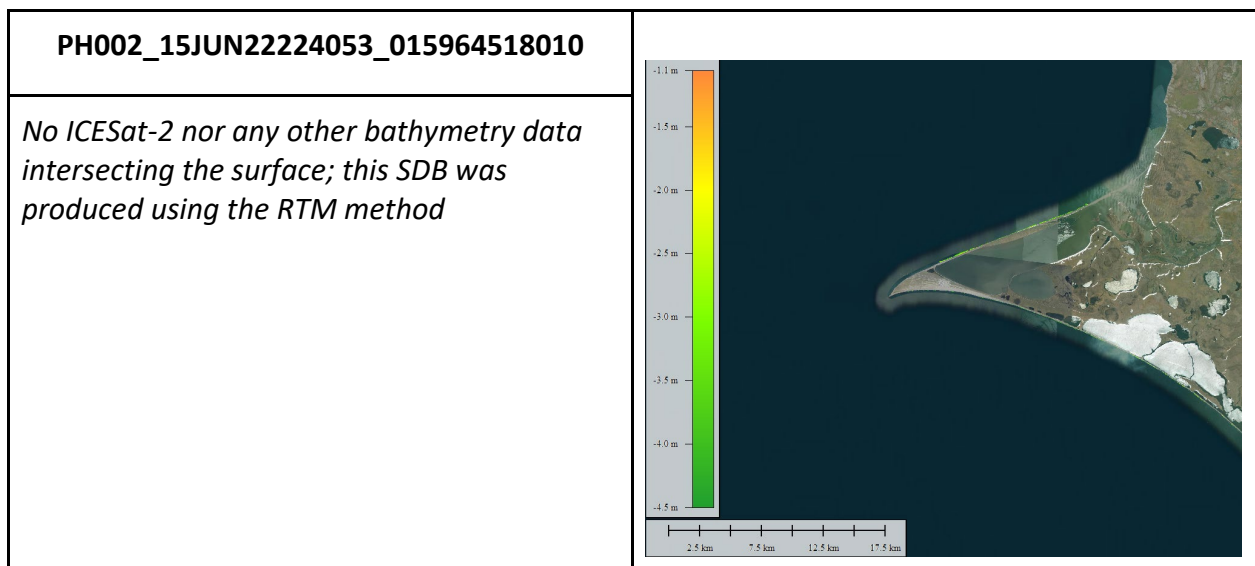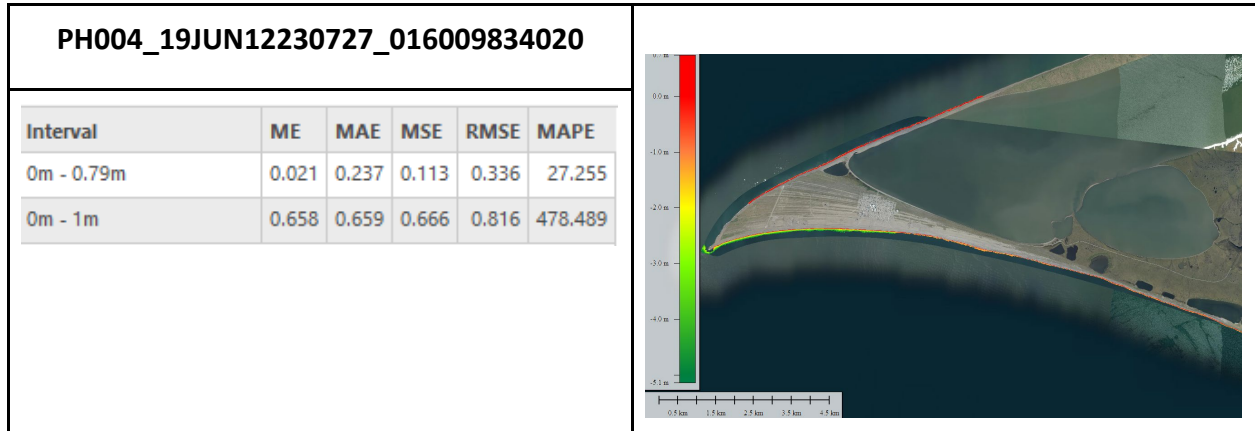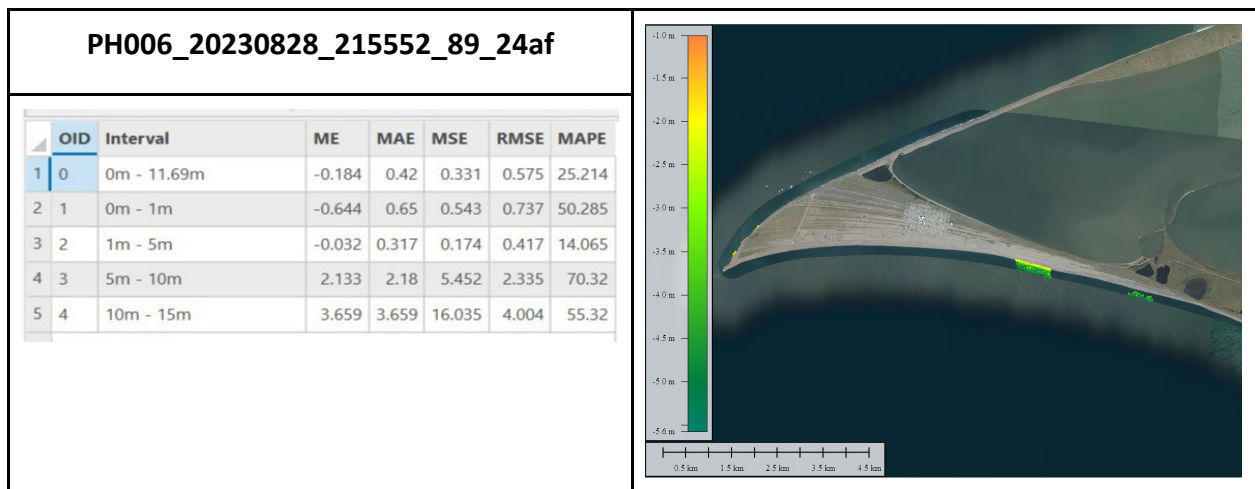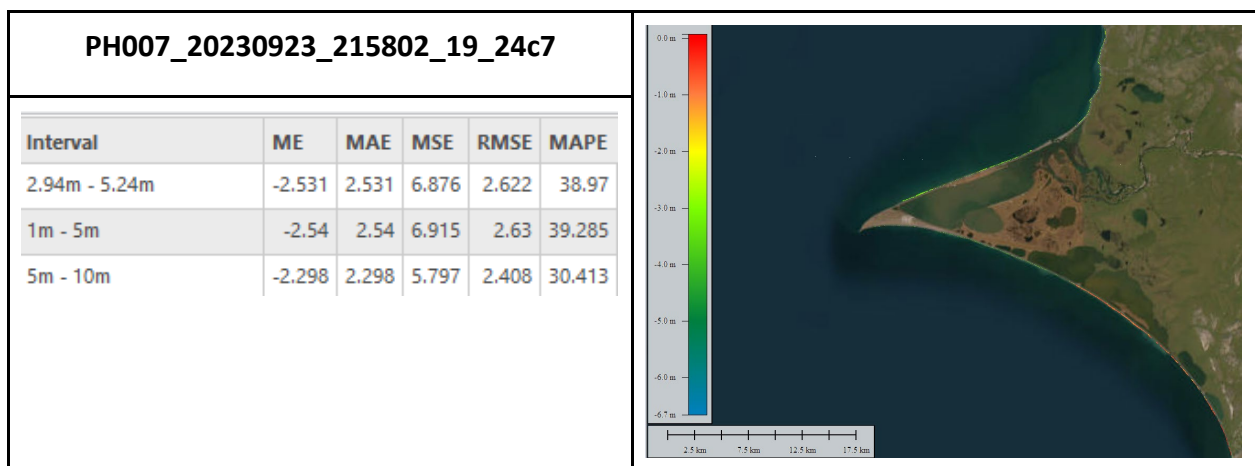| PH007_20230923_215802_19_24c7					
Interval	ME	MAE	MSE	RMSE	MAPE
2.94m - 5.24m	-2.531	2.531	6.876	2.622	38.97
1m - 5m	-2.54	2.54	6.915	2.63	39.285
5m - 10m	-2.298	2.298	5.797	2.408	30.413

Figure 23: *Table of statistical comparison of in-situ bathymetry and PH007 SDB surface (left); Resulting PH007 SDB surface with depths ranging from 0.009m to -6.49m (right)*

1305M223FNCNP0283 – The Generation of a Seamless Topo-Bathy DEM   *NOAA*

4.0 In-situ Data

Available in-situ bathymetry data was downloaded from the National Oceanic and Atmospheric Administration's (NOAA) National Geophysical Data Center (NGDC) and Office for Coastal Management (OCM), Alaska's Elevation Portal (https://elevation.alaska.gov/), and United States Geological Survey's (USGS) repository of Alaska's iFSAR data.

4.1 In-situ Data Acquisition

The table below shows a summary of all the available bathymetry data from the various sources for each AOI. Not all available data was utilized in the DEM due to:

1. Missing depth values in the available files from the data repository
2. Invalid depth values, especially in the single-beam data files

	Kachemak	Teller	Point Hope
Multibeam Bathymetry	22 Surveys	11 Surveys	7 Surveys
Single-beam Bathymetry	0 Surveys	1 Surveys	5 Surveys
Topobathy LiDAR	4 Surveys	1 Surveys	4 Surveys
iFSAR	12 Footprints	14 Footprints	8 Footprints
ICESat-2 Bathymetry	0 Points	23,414 Points	87 Points

Table 10: *Summary of in-situ data that contributed to the DEM products*

4.1.1 Kachemak

The table below shows a summary of individual data that were incorporated into the DEM.

Survey ID	Vertical Datum	Horizontal Datum	UTM Zone	Units	Survey Date Range	Source Institution
H11934	MLLW	NAD 83	5	Meters	2008-08-19 - 2008-08-28	NCEI
H11933	MLLW	NAD 83	5	Meters	2008-08-19 - 2008-08-28	NCEI
H11935	MLLW	NAD 83	5	Meters	2008-08-19 - 2008-09-02	NCEI
H11938	MLLW	NAD 83	5	Meters	2008-07-10 - 2008-09-02	NCEI

Survey ID	Vertical Datum	Horizontal Datum	UTM Zone	Units	Survey Date Range	Source Institution
H12084	MLLW	NAD 83	5	Meters	2008-08-11 - 2008-09-08	NCEI
H12090	MLLW	NAD 83	5	Meters	2009-08-25 - 2009-09-01	NCEI
H12085	MLLW	NAD 83	5	Meters	2009-08-12 - 2009-09-04	NCEI
H12087	MLLW	NAD 83	5	Meters	2009-08-12 - 2009-09-05	NCEI
H12088	MLLW	NAD 83	5	Meters	2009-08-12 - 2009-09-05	NCEI
H12089	MLLW	NAD 83	5	Meters	2009-08-17 - 2009-08-31	NCEI
H09569	MLLW	NAD 27	Projected Polyconic	Meters	1980-05-07 - 1980-08-12	NCEI
H09876	MLLW	NAD 27	Projected Polyconic	Meters	1980-05-09 - 1980-08-12	NCEI
H09877	MLLW	NAD 27	Projected Polyconic	Meters	1980-05-06 - 1981-07-16	NCEI
H09884	MLLW	NAD 27	Projected Polyconic	Meters	1980-06-05 - 1980-08-13	NCEI
H09941	MLLW	NAD 27	Projected Polyconic	Meters	1981-05-13 - 1981-08-21	NCEI
H09893	MLLW	NAD 27	Projected Polyconic	Meters	1980-07-16 - 1980-08-12	NCEI
H09945	MLLW	NAD 27	Projected Polyconic	Meters	1981-06-08 - 1981-08-14	NCEI
H09958	MLLW	NAD 27	Projected Polyconic	Meters	1981-07-11 - 1981-08-19	NCEI
H09940	MLLW	NAD 27	Projected Polyconic	Meters	1981-05-06 - 1981-08-19	NCEI
H09900	MLLW	NAD 27	Projected Polyconic	Meters	1980-07-21 - 1980-08-18	NCEI
H12146	MLLW	NAD 83	5	Meters	2009-09-04-2009-09-08	NCEI

Survey ID	Vertical Datum	Horizontal Datum	UTM Zone	Units	Survey Date Range	Source Institution
H12086	MLLW	NAD 83	5	Meters	2009-09-03-2009-09-08	NCEI
2019 USACE NCMP Topobathy Lidar: Alaska	NAVD88	NAD83	5	Meters	2019	Digital Coast
2018 USACE NCMP Topobathy Lidar: Homer	NAVD88	NAD83	5	Meters	2018	Digital Coast
2008 NOAA NGS Lidar: Kenai Peninsula (AK)	NAVD88	NAD83	5	Meters	2008	Digital Coast
2008 Kenai Watershed Forum Lidar: Kenai Peninsula, AK - 1	NAVD88	NAD83	5	Meters	2008	Digital Coast
IFSAR						
DTM_N5915W15115P	Unknown	NAD83	5	Meters	2014-08-29 - 2014-09-12	DGGS Elevation Portal
DTM_N5915W15130P	Unknown	NAD83	5	Meters	2014-08-29 - 2014-09-12	DGGS Elevation Portal
DTM_N5915W15145P	Unknown	NAD83	5	Meters	2014-08-29 - 2014-09-12	DGGS Elevation Portal
DTM_N5915W15200P	Unknown	NAD83	5	Meters	2014-08-29 - 2014-09-12	DGGS Elevation Portal
DTM_N5930W15100P	Unknown	NAD83	5	Meters	2014-08-29 - 2014-09-12	DGGS Elevation Portal
DTM_N5930W15115P	Unknown	NAD83	5	Meters	2014-08-29 - 2014-09-12	DGGS Elevation Portal
DTM_N5930W15130P	Unknown	NAD83	5	Meters	2014-08-29 - 2014-09-12	DGGS Elevation Portal
DTM_N5930W15145P	Unknown	NAD83	5	Meters	2014-08-29 - 2014-09-12	DGGS Elevation Portal
DTM_N5930W15200P	Unknown	NAD83	5	Meters	2014-08-29 - 2014-09-12	DGGS Elevation Portal
DTM_N5945W15100P	Unknown	NAD83	5	Meters	2014-08-29 - 2014-09-12	DGGS Elevation Portal
DTM_N5945W15115P	Unknown	NAD83	5	Meters	2014-08-29 - 2014-09-12	DGGS Elevation Portal
DTM_N5945W15130P	Unknown	NAD83	5	Meters	2014-08-29 - 2014-09-12	DGGS Elevation Portal

Table 11: *Summary of in-situ topo-bathy data for the Kachemak AOI*

4.1.2 Teller

The table below shows a summary of individual data that were incorporated into the DEM.

Survey ID	Vertical Datum	Horizontal Datum	UTM Zone	Units	Survey Date Range	Source Information
D00226	MLLW	NAD83	3	Meters	2017-07-11 - 2017-09-04	NCEI
H12798	MLLW	NAD83	3	Meters	2017-07-12 - 2017-08-31	NCEI
H07837	MLLW	NAD83	3	Meters	1950-01-01 - 1950-12-31	NCEI
H12800	MLLW	NAD83	3	Meters	2017-07-21 - 2017-08-23	NCEI
H12799	MLLW	NAD83	3	Meters	2017-07-21 - 2017-08-29	NCEI
H12232	MLLW	NAD83	3	Meters	2010-07-19 - 2010-09-02	NCEI
H11273	MLLW	NAD83	3	Meters	2005-06-09 - 2005-08-20	NCEI
H11274	MLLW	NAD83	3	Meters	2005-06-09 - 2005-08-20	NCEI
H07840	MLLW	NAD83	3	Meters	1950-01-01 - 1950-12-31	NCEI
H07838	MLLW	NAD83	3	Meters	1950-01-01 - 1950-12-31	NCEI
H09020	MLLW	NAD83	3	Meters	1968-06-19 - 1968-09-18	NCEI
S576BS	Unknown	Unknown	Unknown	Meters	1976-09-20 - 1976-10-14	NCEI
2019 USACE NCMP Topobathy Lidar: Alaska	NAVD88	NAD83	3	Meters	2019	Digital Coast
IFSAR						
IFSARAKDTM2012N6500W16600_01	NAVD88	NAD83	AlbersConicalEqualArea	Meters	2012-07-06- 2012-07-12	USGS

Survey ID	Vertical Datum	Horizontal Datum	UTM Zone	Units	Survey Date Range	Source Information
IFSARAKDTM2012N6500W16615_01	NAVD88	NAD83	AlbersConicalEqualArea	Meters	2012-07-05-2012-07-12	USGS
IFSARAKDTM2012N6500W16630_01	NAVD88	NAD83	AlbersConicalEqualArea	Meters	2012-07-05-2012-07-12	USGS
IFSARAKDTM2012N6500W16645_01	NAVD88	NAD83	AlbersConicalEqualArea	Meters	2012-07-05-2012-07-12	USGS
IFSARAKDTM2012N6500W16700_01	NAVD88	NAD83	AlbersConicalEqualArea	Meters	2012-07-05-2012-07-12	USGS
IFSARAKDTM2012N6515W16615_01	NAVD88	NAD83	AlbersConicalEqualArea	Meters	2012-07-05-2012-07-12	USGS
IFSARAKDTM2012N6515W16630_01	NAVD88	NAD83	AlbersConicalEqualArea	Meters	2012-07-05-2012-07-12	USGS
IFSARAKDTM2012N6515W16645_01	NAVD88	NAD83	AlbersConicalEqualArea	Meters	2012-07-05-2012-07-12	USGS
IFSARAKDTM2012N6515W16700_01	NAVD88	NAD83	AlbersConicalEqualArea	Meters	2012-07-05-2012-07-12	USGS
IFSARAKDTM2012N6515W16715_01	NAVD88	NAD83	AlbersConicalEqualArea	Meters	2012-07-05-2012-07-10	USGS
IFSARAKDTM2012N6515W16730_01	NAVD88	NAD83	AlbersConicalEqualArea	Meters	2012-07-05-2012-07-10	USGS
IFSARAKDTM2012N6515W16745_01	NAVD88	NAD83	AlbersConicalEqualArea	Meters	2012-07-05-2012-07-10	USGS
IFSARAKDTM2012N6530W16745_01	NAVD88	NAD83	AlbersConicalEqualArea	Meters	2012-07-05-2012-07-10	USGS

Survey ID	Vertical Datum	Horizontal Datum	UTM Zone	Units	Survey Date Range	Source Information
IFSARAKDTM2012N6445W16645_01	NAVD88	NAD83	AlbersConicalEqualArea	Meters	2012-07-04- 2012-07-10	USGS

Table 12: *Summary of in-situ topo-bathy data for the Teller AOI*

TCarta also produced 23,414 ICESat-2 bathymetry points in the Teller AOI. TCarta produced these data in 2022.
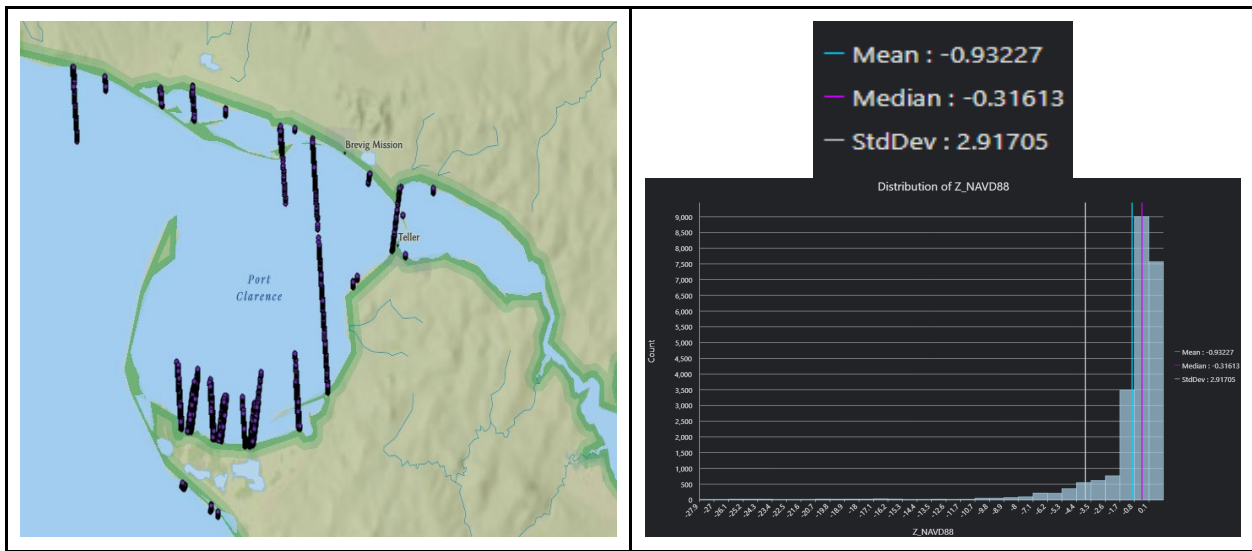

Figure 24: *Available ICESat-2 bathymetry data in Teller (right) and their statistics (left) with a mean of - 0.93m, median of -0.31m, and standard deviation of 2.91m*

4.1.3 Point Hope

The table below shows a summary of individual data that were incorporated into the DEM.

Survey ID	Vertical Datum	Horizontal Datum	UTM Zone	Units	Survey Date Range	Source Information
H13120	MLLW	NAD 83	3	Meters	2018-07-14 - 2018-08-10	NCEI
D00271	MLLW	NAD 83	3	Meters	2020-08-03 - 2020-10-24	NCEI
H13121	MLLW	NAD 83	3	Meters	2018-07-30 - 2018-08-10	NCEI

Survey ID	Vertical Datum	Horizontal Datum	UTM Zone	Units	Survey Date Range	Source Information
H13123	MLLW	NAD 83	3	Meters	2018-07-15 - 2018-08-15	NCEI
H13122	MLLW	NAD 83	3	Meters	2018-07-16 - 2018-08-11	NCEI
D00168	MLLW	NAD 83	2,3, 4,5,6	Meters	2012-08-05 - 2012-08-23	NCEI
L1182CS	Unknown	Unknown	Unknown	Meters	1982-08-27 - 1982-09-16	NCEI
L880AR	Unknown	Unknown	Unknown	Meters	1980-09-04 - 1980-09-20	NCEI
PZ73000	Unknown	Unknown	Unknown	Meters	1973	NCEI
NBP0304A	Unknown	Unknown	Unknown	Meters	2003-07-06 - 2003-08-17	NCEI
EW9410	Unknown	Unknown	Unknown	Meters	1994-08-06 - 1994-09-01	NCEI
2019 USACE NCMP Topobathy Lidar: Alaska	NAVD88	NAD 83	3	Meters	2019	Digital Coast
2018 USGS Lidar: North Slope, AK-QL11	NAVD88	NAD83	3	Meters	2018	Digital Coast
2004 NOAA NGS Lidar: AK Coastline - 1	NAVD88	NAD83	3	Meters	2004	Digital Coast
2018 USGS Lidar: North Slope, AK-QL21	NAVD88	NAD83	3	Meters	2018	Digital Coast
IFSAR						
IFSARAKDTM2012N6800W16615_01	NAVD88	NAD83	AlbersConicalEqualArea		2012-07-21- 2012-07-21	USGS
IFSARAKDTM2012N6815W16615_01	NAVD88	NAD83	AlbersConicalEqualArea		2012-07-21- 2012-07-21	USGS
IFSARAKDTM2012N6815W16630_01	NAVD88	NAD83	AlbersConicalEqualArea		2012-07-21- 2012-07-21	USGS
IFSARAKDTM2012N6815W16645_01	NAVD88	NAD83	AlbersConicalEqualArea		2012-07-21- 2012-07-21	USGS
IFSARAKDTM2012N6815W16700_01	NAVD88	NAD83	AlbersConicalEqualArea		2012-07-21- 2012-07-21	USGS
IFSARAKDTM2012N6830W16630_01	NAVD88	NAD83	AlbersConicalEqualArea		2012-07-21- 2012-07-21	USGS

Survey ID	Vertical Datum	Horizontal Datum	UTM Zone	Units	Survey Date Range	Source Information
IFSARAKDTM2012N6800W16600_01	NAVD88	NAD83	AlbersConicalEqualArea		2012-07-21-2012-07-21	USGS
IFSARAKDTM2012N6830W16615_01	NAVD88	NAD83	AlbersConicalEqualArea		2012-07-21-2012-07-21	USGS

Table 13: *Summary of in-situ topo-bathy data for the Point Hope AOI*

There were also 87 ICESat-2 bathymetry data points available in the Point Hope AOI. TCarta produced these data in 2022.
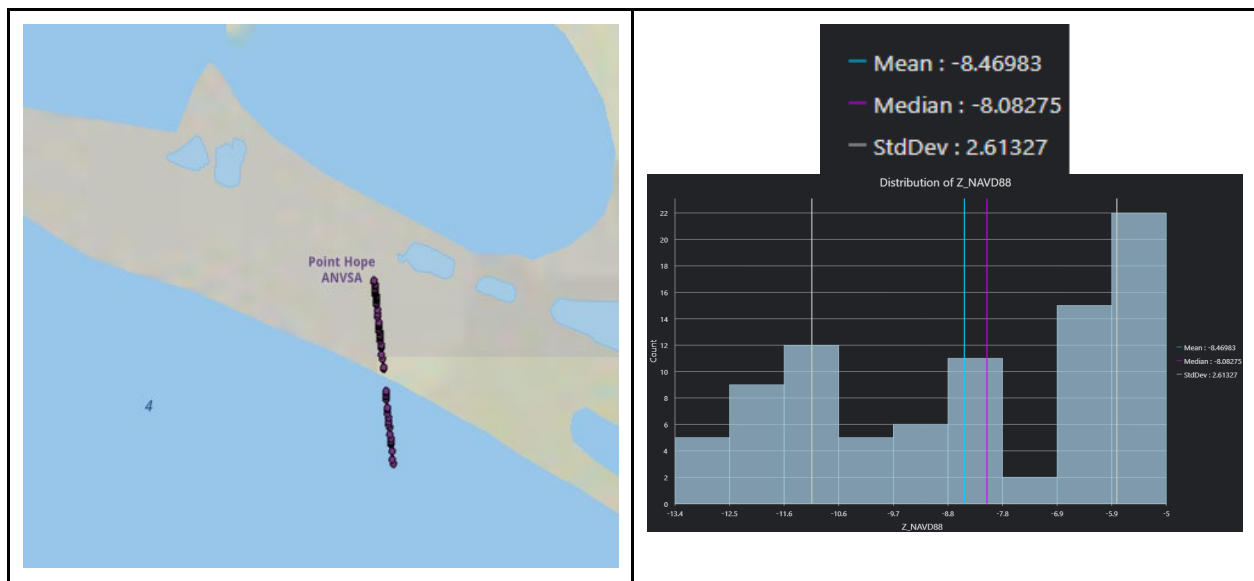
Figure 25: *Available ICESat-2 bathymetry data in Point Hope (left) and their statistics (right) with a mean of -8.46m, median of 8.08m, and standard deviation of 2.61m*

4.2 Data Cleaning

Some of the topobathy LiDAR surveys had erroneous classification and needed to be edited/removed manually to remove spurious data. The LiDAR datasets were parsed based on classification to ensure that only ground and bathymetry data points were utilized, resulting in bare-earth inputs wherever possible. iFSAR data were assessed and points with zero returns over water were taken out. All the available data was then constrained to the AOI extents with a buffer added.

Initial DEM tests were generated at a 5m resolution. An initial visual look at the resulting

surfaces helped pinpoint areas that needed further attention and helped narrow down some of the problematic in-situ bathymetric data. Some of the identified issues were:

- Gridding pattern
- DEM Corduroy
- Irregular triangulation
- Linear and circular features
- Dots in a line
- Zig-zag pattern
- Irregular/inconsistent bathy transition
- Speckled nearshore DEM
- Sonar trackline issue

Each of these observations was individually reviewed to determine the best course of action to correct. In most cases, the observed artifacts were because of disagreements between older, sparse bathymetry surveys and more recent surveys. To correct these issues, a deconfliction algorithm was applied. The algorithm used euclidean distance and vertical delta thresholding to eliminate older points which had greater than 5% depth variation and were proximate to more recent or higher-quality data. This routine allowed for the retention of seafloor morphology, while also reducing artifacts such as gridding patterns or "DEM corduroy". In some instances, the DEM artifacts were inherent to the source bathymetry data itself. Any remnant conditions have been annotated in the known issues feature class polygons, included in the project's geodatabase deliverable. More information on the cleaning process can be found in section 5.3.
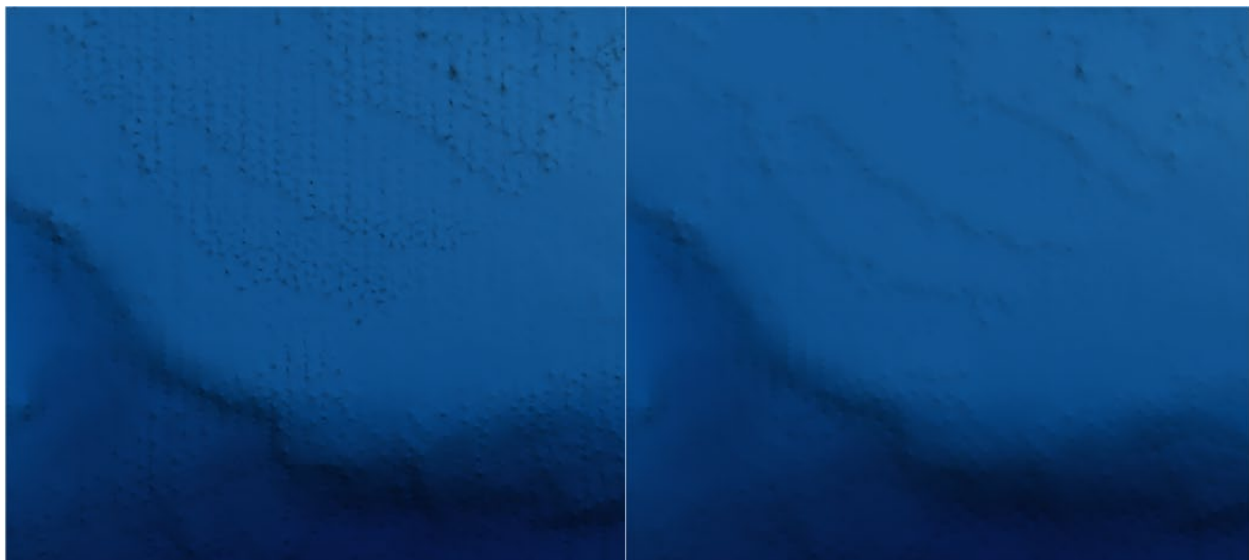

Figure 26: *Kachemak 5m DEM before in-situ deconfliction (left) & Kachemak 2m DEM after deconfliction*

4.3 Datum Transformation

The downloaded data were in different horizontal and vertical coordinate systems. This project was to be delivered in:

- Horizontal Datum: NAD 83 2011, projected to the local UTM zone.
- Vertical Datum: NAVD88 (meters) referenced to GEOID12.

4.3.1 Vertical Datum Transformation

The in-situ data were in different vertical datums, with most of the sonar bathymetry data downloaded from NGDC being in MLLW. There were inherent tide uncertainties associated with these surveys. The uncertainty was dependent on the published values for MSL and mean range of the tide at each utilized tide station within the National Water Level Observation Network (NWLON) during the time the surveys were conducted.

All the in-situ data were first transformed from their resident vertical datum to NAVD88 (referenced to Geoid 12). Unfortunately, the currently available VDatum transformation models do not work for the Alaska exclusive economic zone (EEZ).

An internal Ellipsoidally Referenced Tide Datum Model (ERTDM), based on *Riley et al.,* 2016 work on VDatum for Alaska, was utilized to perform the VDatum transformation from MLLW to NAVD88 (GEOID12). A MLLW - NAVD88 (GEOID 12) triangulated mesh covering all the Alaskan tidal benchmarks was the basis for this model. We received a copy of this mesh from the Coast Survey Development Lab. An initial effort to achieve the creation of such a mesh was futile, as we were constrained to only the few available tidal benchmarks. Using the mesh that covered the whole of Alaska increased the accuracy of the resulting vertical transformation differences.

All the in-situ data was first transformed from its native vertical datum to MLLW, where applicable. The resulting ERTDM was then constrained to the same AOI extent as the in-situ data and the vertical datum transformation was done. To achieve this, the mesh was interpolated using a triangle interpolation method which respected the boundary conditions of the mesh, while allowing for interstitial values to be resolved. With this interpolated mesh, all MLLW values were intersected and the value of the MLLW-NADV88 TSS correction was applied to convert the vertical datum of each in-situ point, as needed.

4.3.2 Horizontal Datum Transformation

The datasets, which had been corrected to NAVD88, were then transformed to NAD83 (2011) and projected to their respective UTM Zone: Kachemak ~ 5N, Teller ~ 3N, and Point Hope ~ 3N.

5.0 Gridding

For the initial interim 5m DEM delivery, TCarta utilized NOAA's Continuously Updated Digital Elevation Model (CUDEM) software, an open-source python ecosystem for producing DEMs. However, this system's primary capabilities center upon acquiring and preparing data from various sources, which was not relevant for this project, given the specific requirements for vertical datum adjustment, and the inclusion of SDB. To ensure expedient processing, and iterative DEM improvements for 2m DEM creation, TCarta elected to implement a custom python-driven pipeline for aggregating, weighting, and interfacing with the interpolation algorithm directly. This accomplished the same process as the CUDEM python library; while CUDEM invoked the same open-source interpolation software, the custom pipeline allowed for more finite control over data integration, coincident in-situ weighting mechanisms, and interpolation parameters.

5.1 Data Grading

Individual data types were assigned weights based on source sensor/provenance and date of collection. All the data was then combined to a singular in-situ grid at the DEM resolution, where coincident points from multiple sources were averaged based on their assigned weights.

5.2 Data Interpolation

The weighted in-situ grid was interpolated utilizing the open-source Generic Mapping Tools (GMT) surface adjustable tension continuous curvature splines algorithm *[Smith et al., 1990]*. Several iterations were run with different tension and convergence values to achieve minimal deviation from known data points, while limiting spurious or outlier interpolated values. Given the relatively sparse in-situ data in some areas of the project domains, relative to the target DEM resolution of 2m, a high-tension value of 0.8 - 0.875, relaxation factor of 1.0, and iterations between 8,000 and 10,000, produced the best results.

5.3 DEM Analysis and Editing

Several iterative interpolation runs were performed for each AOI. After each run, the intermediate DEMs were evaluated for both interpolation quality and for the integration/interaction between overlapping or adjacent in-situ sources. When observed, issues with interpolation, such as overfitting, outlier curvatures, or other interpolation artifacts were mitigated by manipulating interpolation parameters such as tension, relaxation or interpolation

iteration count. For issues with imbricate or adjacent in-situ sources, two primary hierarchical mitigation processes were applied. The primary mechanism was to adjust the weights applied to overlapping data sources to suppress outlier data and/or enhance more quality data. Where data did not overlap, further manual removal of outlier data points, or re-introduction of previously removed data was used to reduce artifacts. While every effort was made to reduce DEM issues, some do remain for various reasons, including visual artifacts due to the intersection of SDB and MBES data, where the texture of the surface is incongruent, but the vertical accuracy of the two data sources is within expected ranges. Additionally, there is some uncertainty surrounding the above/below water status of intertidal areas or mudflats. Finally, some data sources have slight discrepancies, but removal of the data would greatly increase the area of interpolation, and the seafloor model quality would be reduced. All existing known issues are annotated in each AOI's polygon feature class in the provided file geodatabase. Please note that the polygons and associated remarks are representative of existing conditions and do not necessarily delineate every instance of the attributed issue or characteristics.
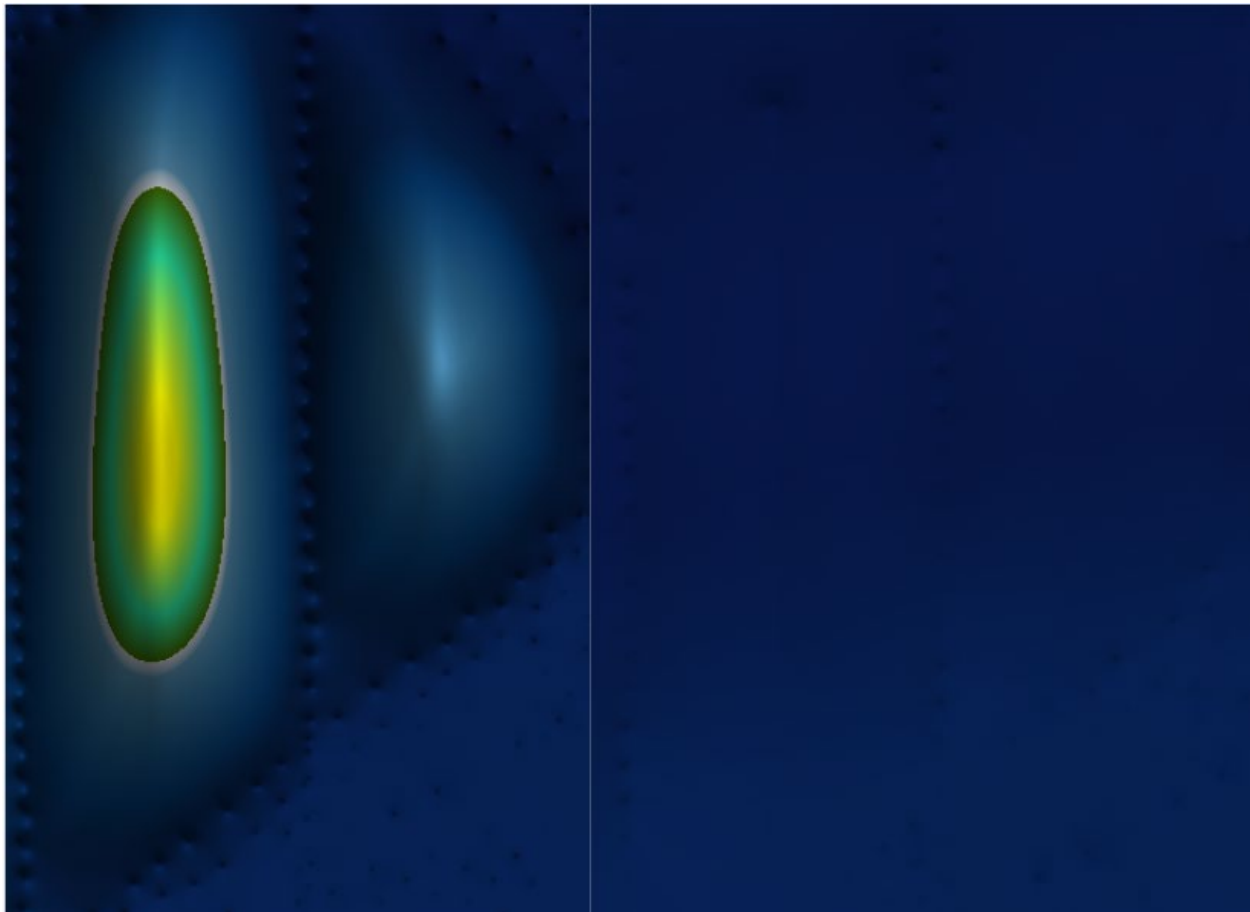

Figure 27: *Kachemak 2m DEM interpolation artifact before correction (left) and after interpolation parameter adjustment (right)*

5.4 Quality Control

To assess the vertical accuracy of the DEMs, a set of 3,000 randomly sampled points from each AOI's non-SDB bathymetry sources were collected. The elevation of each point was compared to the coincident DEM elevation, deriving absolute error, and absolute percent error.

From these point statistics, an overall assessment of vertical accuracy was established, with three key metrics: MAE, RMSE, and MAPE.

AOI	Vertical Accuracy Statistics			Sample Elevation (NAVD88)	
	MAE (m)	RMSE (m)	MAPE (%)	Min (m)	Max (m)
Kachemak	0.52	1.17	5.1	-166.0	+1.88
Teller	0.24	0.51	5.22	-46.65	-4.0
Point Hope	0.06	0.12	0.32	-16.32	+0.32

Table 14: *Summary of vertical accuracy statistics from sample data in each AOI*

6.0 Vertical and Horizontal Control

6.1 Vertical Control

The vertical datum for this project is the North American Vertical Datum of 1988 (NAVD 88) (meters) referenced to GEOID12. The chart to ellipsoid datum transformation was done using an internally developed ERTDM, as described in section 4.3.

6.2 Horizontal Control

The horizontal datum for this project is the North American Datum of 1983 (NAD 83). The projection used for this projection is Universal Transverse Mercator (UTM) Zone 5 for Kachemak and Zone 3 for Teller and Point Hope.

7.0 Results and Recommendations

7.1 Results

Information on the morphology of the seafloor is crucial for the monitoring of seafloor changes, sediment transport, seafloor spreading, modeling of ice sheets, study of the ocean circulation, and navigation. The resulting DEMs will prove crucial to the communities in Kachemak, Teller, Point Hope, and the state of Alaska as a whole.

7.1.1 Kachemak

A total of 13.54km² of SDB was produced for the Kachemak AOI. This was then gridded with other in-situ bathymetry and topography data available in the area to produce a two-meter seamless DEM covering a total area of 1012.74km².
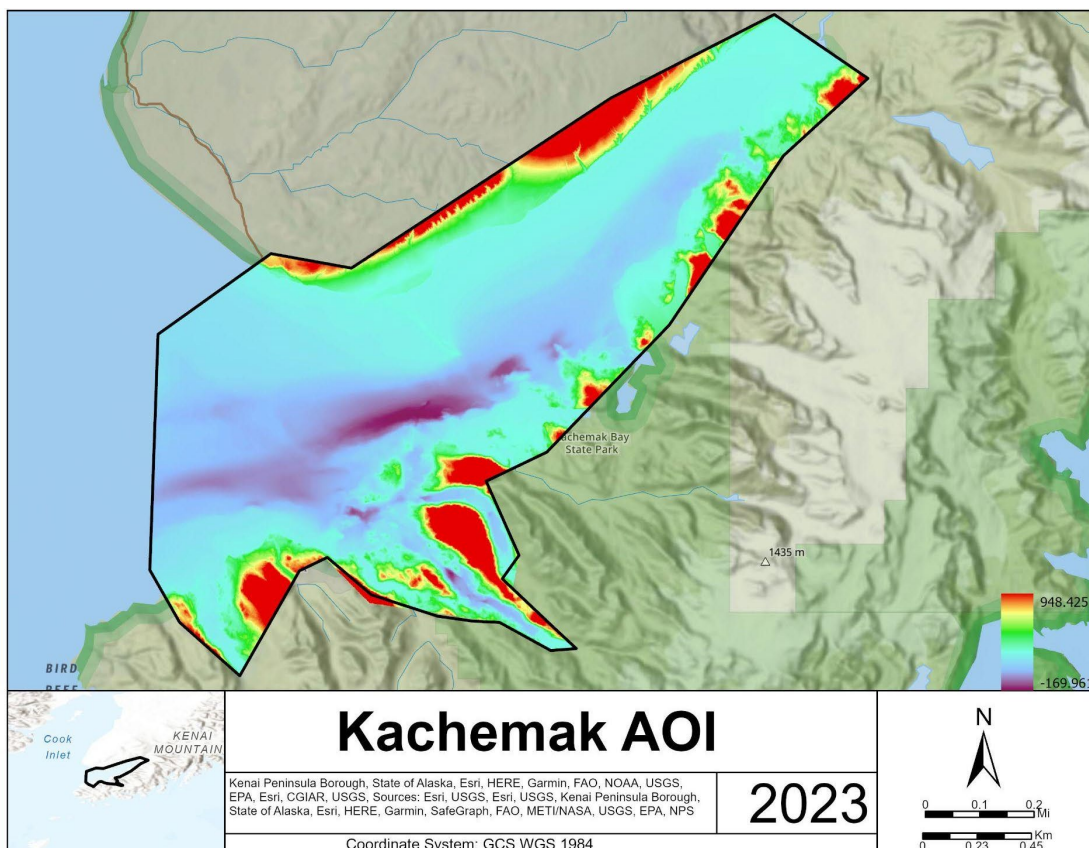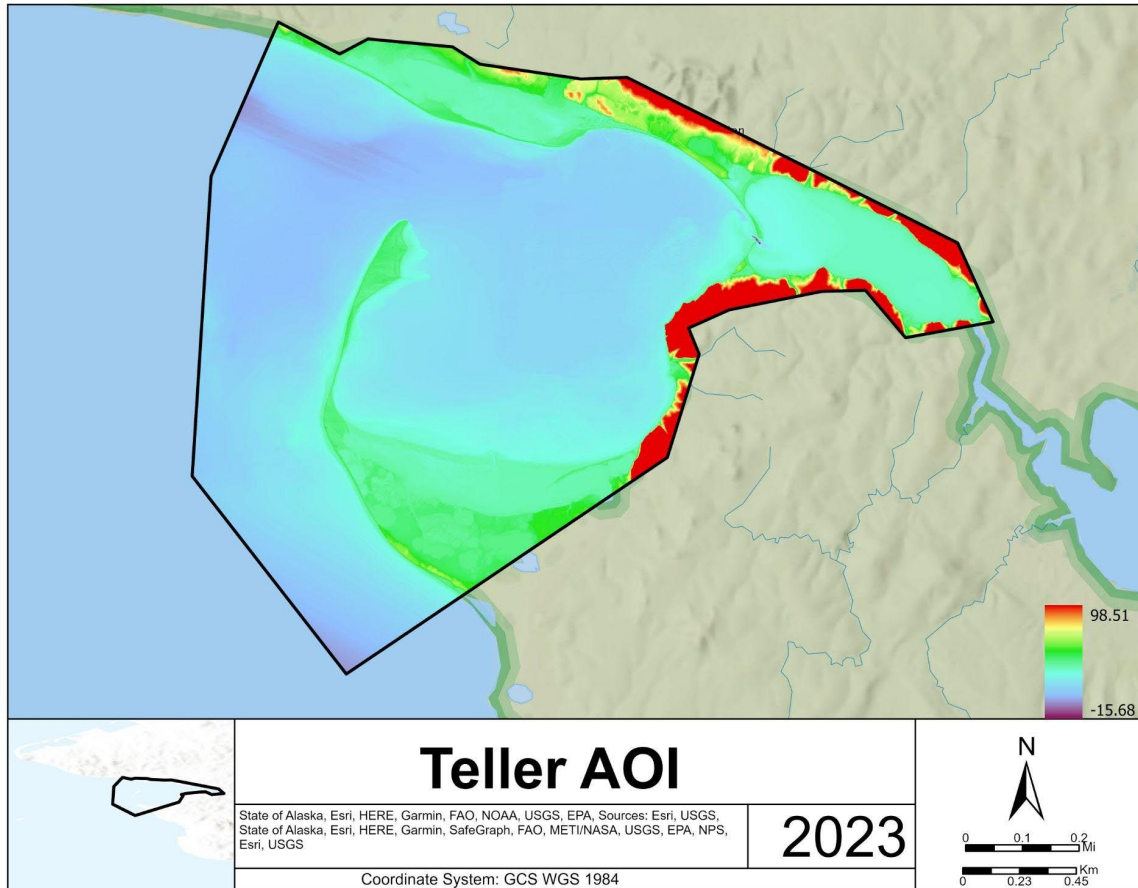

Figure 28: *Kachemak 2m DEM*
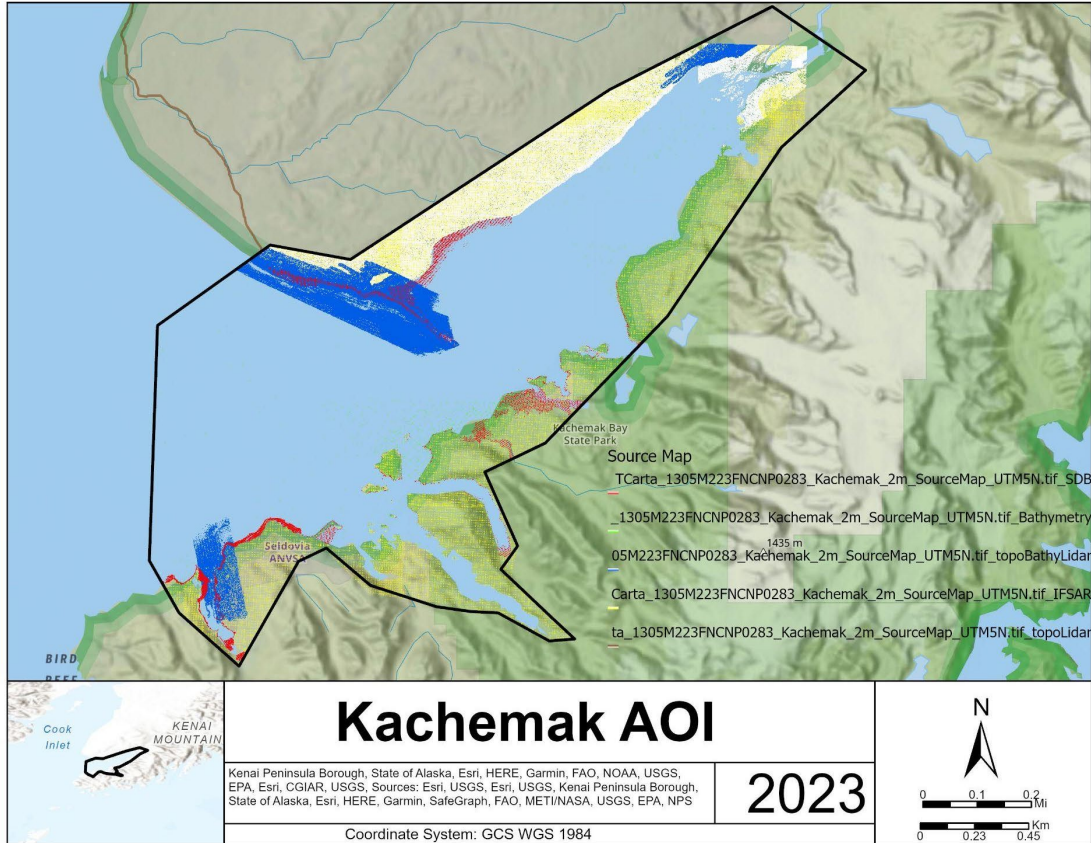
Figure 29: *Data source map showing the contributing datasets to the Kachemak DEM*

7.1.2 Teller

A total of 162.26km² of SDB was produced for the Teller AOI. This was then gridded with other in-situ bathymetry and topography data available in the area to produce a two-meter seamless DEM covering a total area of 1160.69km².
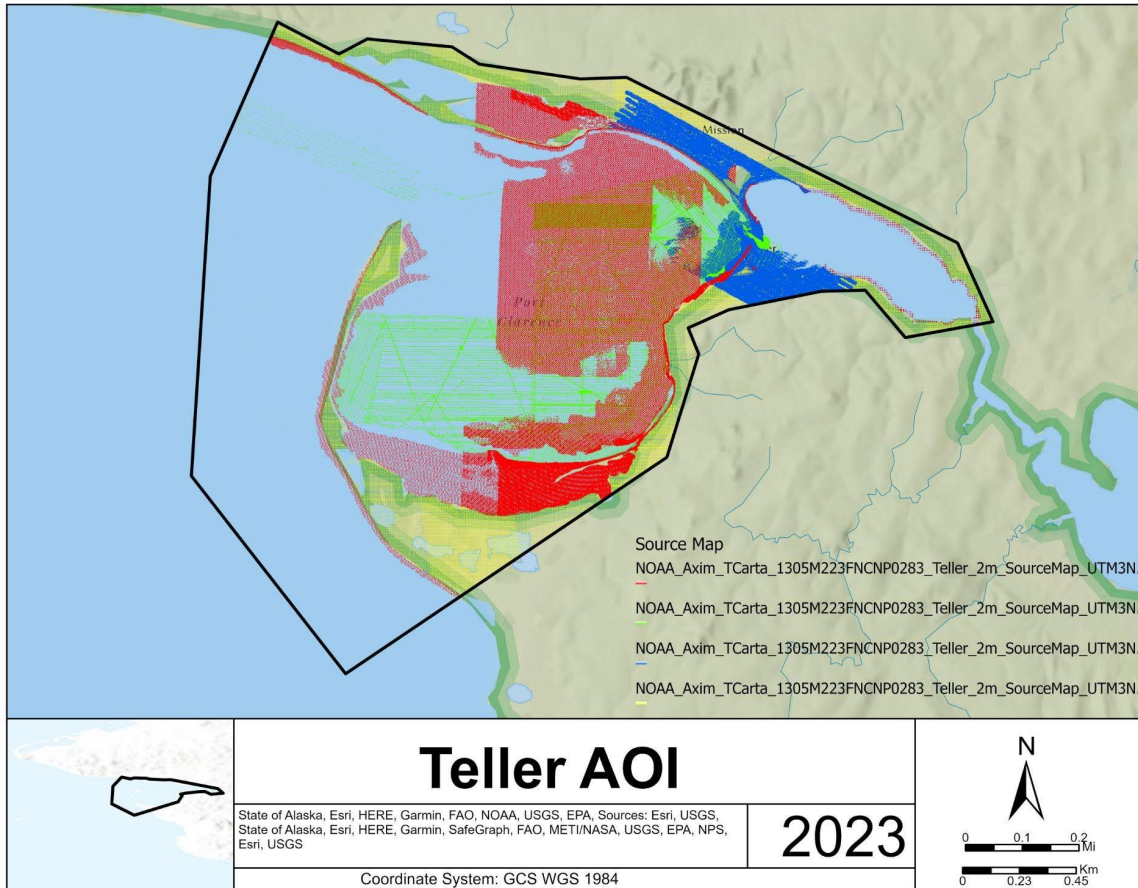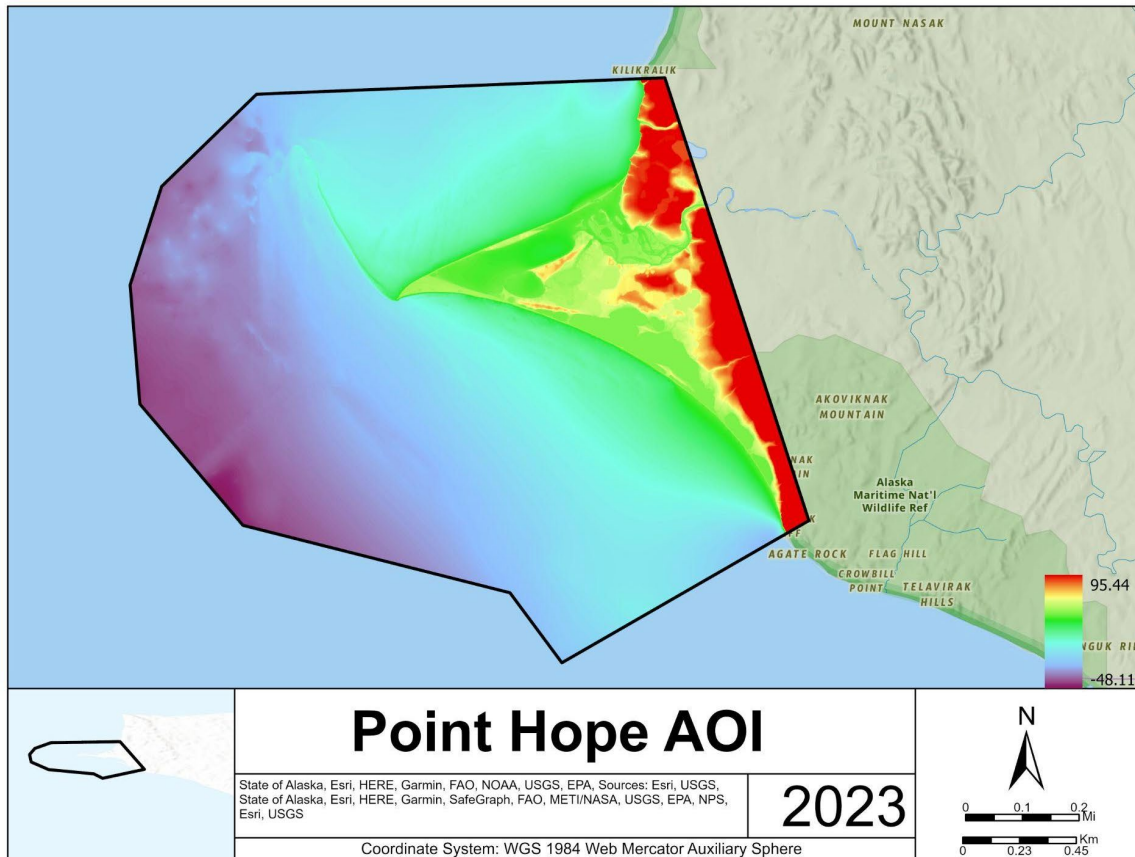

Figure 30: *Teller 2m DEM*

Figure 31: *Data source map showing the contributing datasets to the Teller DEM*

7.1.3 Point Hope

A total of 1.84km² of SDB was produced for the Point Hope AOI. This was then gridded with other in-situ bathymetry and topography data available in the area to produce a two-meter seamless DEM covering a total area of 2292.28km².
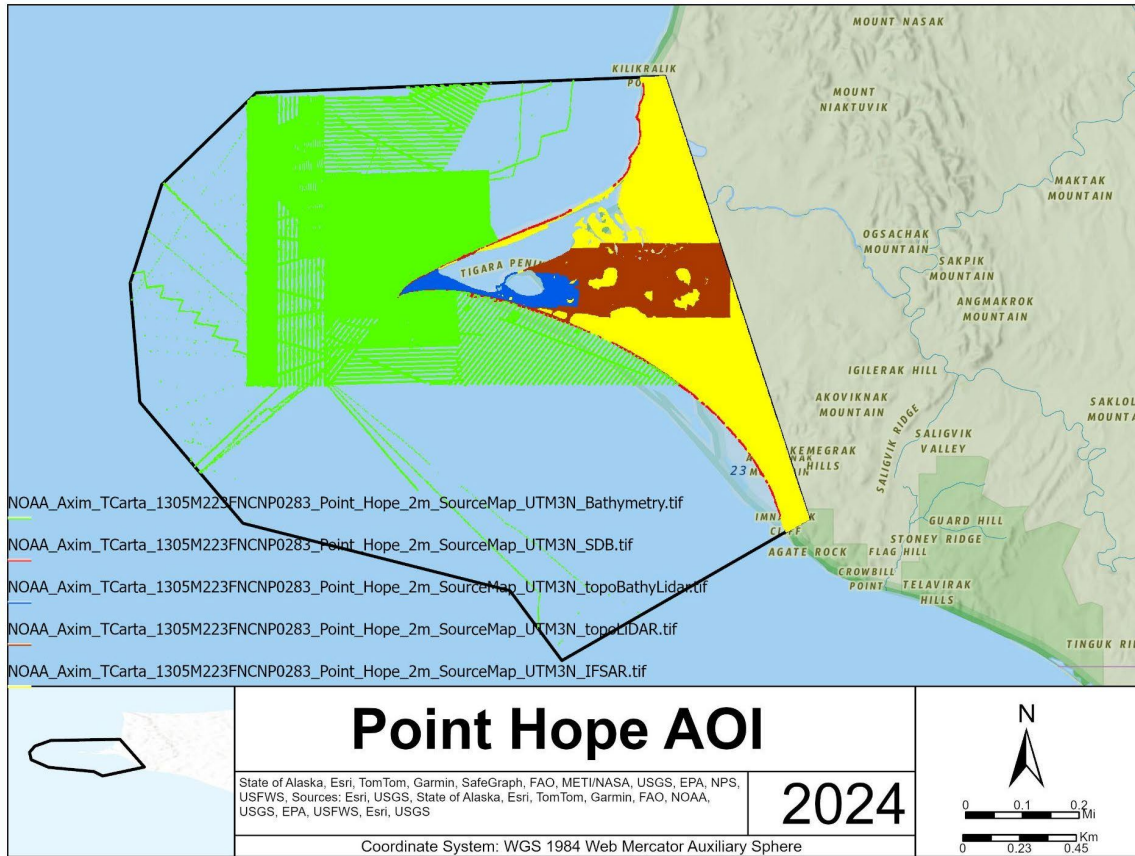

Figure 32: *Point Hope 2m DEM*

Figure 33: *Data source map showing the contributing datasets to the Teller DEM*

7.2 New Survey Recommendations

The assessment for potential areas in Alaska that would benefit from similar DEM generation was based on availability of ICESat-2 and other in-situ bathymetry data, and imagery that could be utilized to generate SDBs. SDB production in these areas would help mitigate the limitations imposed on ship-based and LiDAR surveys due to the remoteness of these areas, cost, and limited data acquisition times due to environmental and weather conditions. SDB on the other hand would offer an opportunity for regular data acquisition at a reasonable cost. Satellites can also be tasked to collect data at set times when environmental and weather conditions are predicted to result in the best imagery, while keeping the cost relatively low.

The ICESat-2 profiles shown in each recommended area were also part of the 2022 TCarta effort to acquire ICESat-2 bathymetry data for the whole of Alaska. This effort resulted in ~300,000 bathymetry points collected. TCarta has found that ICESat-2 returns indicate feasibility for SDB in an area. These areas include, but are not limited to:

7.2.1 Katalla

SDB is feasible in small areas of Katalla Bay and Fox Island. However, areas south of Kanak Island to Okalee Channel are potential for SDB production. Sandbanks to the east of Wingham Island are great locations for SDB. Farther South, off the west shore of Kayak Island, there is visible seafloor nearly six kilometers into the Bay of Alaska.

Figure 34: *A visual representation of available ICESat-2 bathymetry data in Katalla (left); A sample image to be utilized for SDB production (right)*

7.2.2 Cordova

In the areas closest to Cordova, from Odiak Slough out to the sandbar South of Spike Island, are great locations for SDB production. When expanding the scope, almost all of Orca Inlet is feasible for SDB. This is advantageous due to the dynamic nature of the sandbars in the Inlet.

Figure 35: *A visual representation of available ICESat-2 bathymetry in Cordova (left); A sample image to be utilized for SDB production (right)*

7.2.3 Kotzebue Sound

While most of Kotzebue Sound presents as potential AOI for SDB production, the only areas that are feasible for large-scale SDB are on the western side of the Sound, South of Cape Eisenberg, and the eastern side of the Sound, near Kotzebue. On the southern shores of the Sound, there is feasibility in small locations close to Deering.
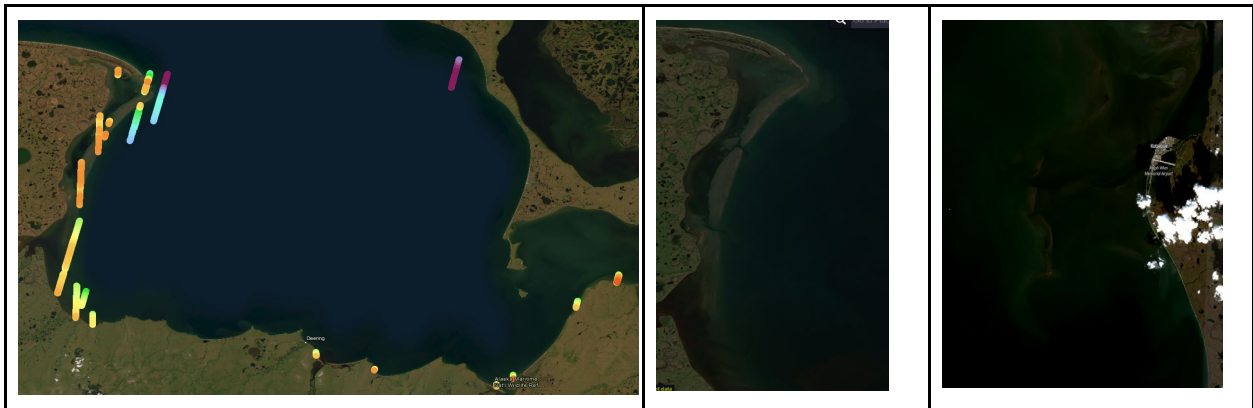

Figure 36: *A visual representation of available ICESat-2 bathymetry in Kotzebue Sound (left); sample images to be utilized for SDB production (center & right)*

7.2.4 Norton Sound

SDB production is feasible along most of the northern shore of Norton Sound, from Nome to Shaktoolik. While the extent of where SDB is feasible varies along the shore, SDB is feasible semi consistently out to about half a kilometer offshore. The waters right off the coast of

Shaktoolik are very turbid, but clear imagery shows feasibility for SDB from Shaktoolik to Cape Denbigh.
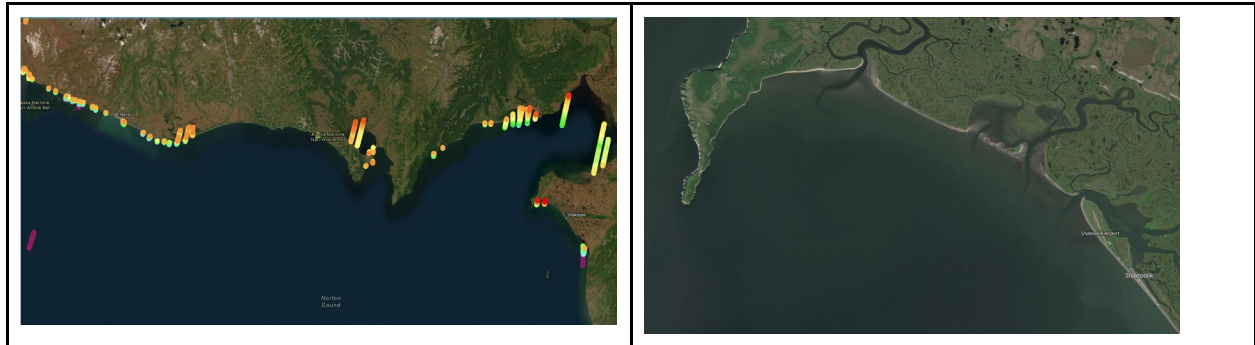

Figure 37: *A visual representation of available ICESat-2 bathymetry in Norton Sound (left); A sample Image to be utilized for SDB production (right)*

7.2.5 Bristol Bay

There are many locations in Bristol Bay for localized SDB production, despite the amount of turbidity in the area. Much of the seafloor off the coast of Togiak, areas around islands in the bay and shallow waters off the coast of Nushagak Peninsula are feasible for SDB. A deeper or more localized investigation might yield different results, but nearly the whole northern shore of the Alaskan peninsula is too turbid for SDB.

7.2.6 Shishmaref

The sandbanks South of Shishmaref and shallow water in Shishmaref inlet can be mapped and monitored for changes using SDB.
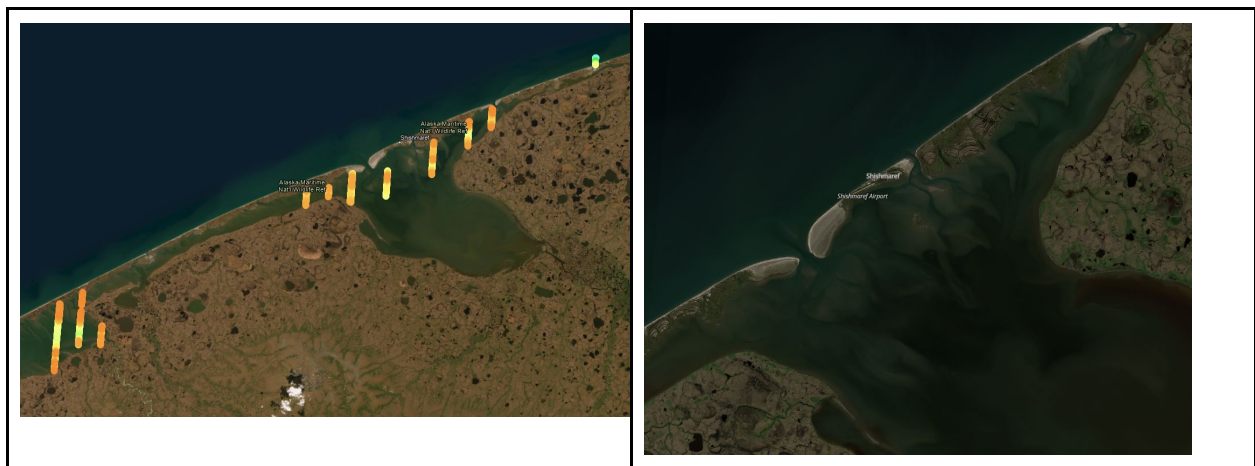

Figure 38: *A visual representation of available ICESat-2 bathymetry in Shishmaref (left); A sample Image to be utilized for SDB production (right)*

7.2.7 Golovin Lagoon

There are lots of opportunities for SDB in Golovin Bay. Optically shallow waters can be seen as South as Cape Darby and Rocky Point. Golovin Lagoon is generally turbid from the Niukluk River delta, but SDB is still feasible throughout the whole AOI.

Figure 39: *A visual representation of available ICESat-2 bathymetry in Golovin Lagoon (left); A sample image to be utilized for SDB production (right)*

References

1. Hedley, J. D., Harborne, A. R., & Mumby, P. J. (2005). Technical note: Simple and robust removal of Sun Glint for mapping shallow-water benthos. *International Journal of Remote Sensing*, *26*(10), 2107–2112. https://doi.org/10.1080/01431160500034086

2. Jakobsson, M., Calder, B., & Mayer, L. (2002). On the effect of random errors in gridded bathymetric compilations. *Journal of Geophysical Research: Solid Earth*, *107*(B12). https://doi.org/10.1029/2001jb000616

3. Ahola, R., Chénier, R., Horner, B., Faucher, M.-A., & Sagram, M. (2018). Satellite derived bathymetry for Arctic charting: A review of sensors and techniques for operational implementation within the Canadian Hydrographic Service. *Remote Sensing of the Ocean, Sea Ice, Coastal Waters, and Large Water Regions 2018*. https://doi.org/10.1117/12.2324965

4. Riley, J. L., Wood, D., & Greenaway, S. (2016). The ellipsoid-referenced zoned datum: A poor man's VDATUM for NOAA Hydrography in Alaska… https://nauticalcharts.noaa.gov/learn/docs/ellipsoidally-referenced-surveys/riley-greenaway-wood-poor-mans-vdatum.pdf

5. Smith, W. H., & Wessel, P. (1990). Gridding with continuous curvature splines in tension. *GEOPHYSICS*, *55*(3), 293–305. https://doi.org/10.1190/1.1442837